



# FINAL PUBLISHABLE JRP REPORT

JRP-Contract number	SIB60	
JRP short name	Surveying	
JRP full title	Metrology for long distance surveying	
Version numbers of latest contracted Annex Ia and Annex Ib against which the assessment will be made	Annex Ia: V1.2	
	Annex Ib: V1.01	
Period covered (dates)	From 01 July 2013	To 30 June 2016
JRP-Coordinator		
Name, title, organisation	Dr. Florian Pollinger, PTB	
Tel:	+49 531 592 5420	
Email:	<a href="mailto:florian.pollinger@ptb.de">florian.pollinger@ptb.de</a>	
JRP website address	<a href="http://www.emrp-surveying.eu">www.emrp-surveying.eu</a>	
Other JRP-Partners		
Short name, country	CNAM, France NLS, Finland INRIM, Italy IPQ, Portugal VTT, Finland RISE, Sweden VSL, Netherlands NSC-IM, Ukraine	
REG1-Researcher (associated Home Organisation)	Steffen Schön (LUH )	Start date: 1 Sep 2013 Duration: 28 months
REG2-Researcher (associated Home Organisation)	Wolfgang Niemeier (TUBS)	Start date: 1 Jan 2014 Duration: 28 months
REG3-Researcher (associated Home Organisation)	Heiner Kuhlmann (UBO)	Start date: 1 Sep 2013 Duration: 28 months
REG4-Researcher (associated Home Organisation)	Nandini Bhattacharya (TU Delft)	Start date: 1 Jan 2014 Duration: 30 months
RMG1-Researcher (Guestworking Organisation)	Adam Lesundak (ISI)	Start date: 1 Feb 2014 Duration: 8 months
RMG2-Researcher (Guestworking Organisation)	Alen Bosnjakovic (IMBiH)	Start date: 1 Jan 2014 Duration: 7 months

**Report Status: PU Public**



TABLE OF CONTENTS

1	Executive Summary .....	3
2	Project context, rationale and objectives.....	9
3	Research results .....	11
3.1	The optical distance measurement in air .....	11
3.1.1	<b>The TeleYAG system as novel primary standard for baseline calibrations.....</b>	<b>11</b>
3.1.2	<b>The TeleDiode System as novel transfer standard .....</b>	<b>13</b>
3.1.3	<b>Air index investigations by long distance spectroscopic thermometry .....</b>	<b>15</b>
3.1.4	<b>Turbulence and optical distance measurement.....</b>	<b>16</b>
3.1.5	<b>Conclusions.....</b>	<b>17</b>
3.2	GNSS-based distance metrology.....	19
3.2.1	<b>GNSS based distance metrology using common clocks .....</b>	<b>19</b>
3.2.2	<b>Tropospheric influence and the combination of long and short baseline solutions.....</b>	<b>20</b>
3.2.3	<b>Influence of the first 50 cm.....</b>	<b>21</b>
3.2.4	<b>Obstruction .....</b>	<b>22</b>
3.2.5	<b>Optimum processing strategy for field measurements .....</b>	<b>23</b>
3.2.6	<b>Conclusions.....</b>	<b>24</b>
3.3	Femtosecond laser-based long distance metrology .....	25
3.3.1	<b>Approaches to mode filtering .....</b>	<b>25</b>
3.3.2	<b>Homodyne many-wavelength interferometry over macroscopic distances .....</b>	<b>26</b>
3.3.3	<b>Heterodyne frequency-comb based interferometry .....</b>	<b>27</b>
3.3.4	<b>Comb-based spectroscopic refractivity compensation .....</b>	<b>28</b>
3.3.5	<b>Conclusions.....</b>	<b>29</b>
3.4	Immediate contributions to surveying practice.....	30
3.4.1	<b>Field inter-comparison of instruments and baselines .....</b>	<b>30</b>
3.4.2	<b>Data digging at the PTB 600 m baseline.....</b>	<b>30</b>
3.4.3	<b>EDM calibration on baselines .....</b>	<b>31</b>
3.4.4	<b>The revolver test field concept for antenna parameter verification.....</b>	<b>31</b>
3.4.5	<b>Good practice guides for high accuracy GNSS-based distance measurements .....</b>	<b>32</b>
3.4.6	<b>Conclusions.....</b>	<b>33</b>
3.5	Local tie metrology at geodetic fundamental stations .....	34
3.5.1	<b>Uncertainty assessment of local tie networks .....</b>	<b>34</b>
3.5.2	<b>Local-tie adapted 3D metrology.....</b>	<b>35</b>
3.5.3	<b>GNSS-VLBI baseline measurement.....</b>	<b>36</b>
3.5.4	<b>Conclusions and outlook .....</b>	<b>36</b>
3.6	Summary of major research results and project outputs .....	38
4	Actual and potential impact.....	39
5	Website address and contact details .....	41
6	List of publications.....	41
7	References.....	45

## 1 Executive Summary

### Overview

Landslides, sinkholes, and other tectonic activities may threaten populations, buildings, or industrial facilities in mining regions, mountain areas and around nuclear plants. Many of these critical sites are therefore monitored for small ground changes by surveyors, who face the challenge of measuring distances over several hundreds of metres to kilometers with uncertainties at less than a millimeter level. For example, when monitoring the stability of critical sites such as nuclear power stations or areas threatened by landslides, surveyors try to detect measurement changes smaller than a millimeter over a year. However, for distances of several hundreds of metres, environmental effects such as temperature, air pressure or local satellite obstruction limit the measurement uncertainty to the order of one millimeter for even the best state-of-the-art devices.

This project addressed the traceability of the two fundamental technologies in surveying: optical and global navigation satellite systems (GNSS) based distance measurements. Novel standards and technologies were developed by the project, leading to a better understanding of uncertainty contributions at the millimeter and sub-millimetre levels, and to a substantial reduction in the levels of uncertainty in length measurements in surveying and geodesy - the accurate study of the Earth's shape and size.

### Need for the project

It is necessary to be able to measure distances up to kilometres with an accuracy of less than one millimetre in many applications. Such applications include, when constructing and monitoring current and future long-distance tunnel projects and the gigantic accelerator facilities used in high energy physics, when establishing local ties between different geodetic instruments on geodetic fundamental stations, and when monitoring deformation networks at critical sites like nuclear power plants or future carbon dioxide repositories.

Many of these critical sites are monitored for tectonic changes by surveyors. For this monitoring, distance measurements in a network of permanent reference points looking for changes over time are often used. For long-term comparability of data points, traceability to the SI definition of the metre is essential and a substantial improvement of the level of measurement uncertainty to the sub-millimetre level would help early decision making.

Due to uncontrollable environmental effects, both the optical and the GNSS approaches to distance measurement are currently unable to achieve traceability to the SI definition of the metre with the required uncertainty.

The accuracy of the optical method, using electronic distance meters (EDMs), also suffers from insufficient determination of the environmental conditions such as the effective temperature within the whole beam path over distances of hundreds of metres. As a consequence, the refractive index cannot not be determined accurately enough to derive the geometric length from the observed optical path length.

GNSS-based distance measurements are influenced by various effects. The electromagnetic properties of the receiver antennas can play an important role – the location of the reference point varies with each antenna, and can depend on the reception angle. Environmental effects such as signal transmission delays in the ionosphere and troposphere, signal reflections by the ground or the local environment, or local satellite visibility effects can also influence the achievable measurement accuracy.

Further to this, space geodetic observations are highly critical for earth science observations and for the maintenance of the global and local GNSS reference system. Space geodetic observations and their spatial correlation (so-called "local tie vectors") at geodetic fundamental stations are distributed all over the world. However, real-time 3D surveying methods and appropriately optimised measurement strategies are required to substantially improve the uncertainty of GNSS based measurements.

Finally, in order to improve daily monitoring work in the field, it is important to offer realistic good practice guidance for state-of-the-art surveying. This includes field-capable optical standards for long-distance baseline calibrations and revised guidelines for the calibration of both EDM and GNSS-based distance meters.

This project addressed these challenges through new and improved methods and guidance. It set out to reduce the uncertainty of long-distance metrology for measurements up to 1 kilometre and to develop traceability to the SI. As part of this novel technological and methodical solutions for calibration and long-distance measurement were developed.

### Scientific and technical objectives

To address the requirements outlined above, the project aimed to improve long-distance measurement methods by:

1. Improving optical measurements in air. In particular, the inline compensation of the refractive index along the whole beam path, and the impact of turbulences on the measurement, with a target relative uncertainty of  $10^{-7}$  over a distance of 1 km.
2. Gaining a better understanding of the uncertainty of GNSS-based distance metrology. This will allow the development of a sound uncertainty model and an optimised field calibration procedure, targeting absolute uncertainties of 1 mm or better.
3. Developing concepts for the application of femtosecond laser-based many-wavelength interferometry to long-distance metrology with a targeted relative measurement uncertainty significantly better than  $4 \times 10^{-7}$  under controlled environments.
4. Developing solutions to improve state-of-the-art surveying practice, ranging from field-capable optical standards with relative uncertainties of  $10^{-7}$  for long-distance baseline calibrations, over refined guidelines for the calibration of both EDM and GNSS-based distance meters, up to an extensive inter-comparison of major primary geodetic baselines in Europe.
5. Investigating different approaches to real-time monitoring of local ties at geodetic fundamental stations, both experimentally and theoretically. Thus, fundamental metrology for the Global Geodetic Observing System (GGOS) will be developed with an overall target to reduce the uncertainty of reference frames to 0.1 mm.

### Results

#### 1. Optical measurements in air with a targeted measurement uncertainty of $10^{-7}$ over a distance of 1 km

In surveying, optical measurements are typically performed under uncontrollable environmental conditions and therefore the accuracy of the measurement of these environmental quantities is limited. In practice, uncertainties below 1 K (kelvin) are only achievable under very stable conditions meaning that prior to the start of the project optical distance measurements were limited to a corresponding uncertainty of 1 mm (i.e.  $10^{-6}$ ) over 1 km distance.

This project developed optical methods suitable for use in the field that were capable of overcoming these limitations. One method used spectroscopy to build an optical thermometer, which was used to measure a temperature resolution below 300 mK over more than 800 m for averaging times of 120 s. The data can then be used to correct optical distance measurement data leading to uncertainties below 0.3 mm over this distance for the influence of the refractive index.

The project also developed devices for distance measurement in air that compensate for the index of refraction simultaneously with the distance measurement. The devices were based on an idea developed in the 1960s i.e. that if you measure a distance with two well-known optical frequencies and roughly determine the humidity, no further temperature or air pressure data is needed to derive the distance. The two devices were: the TeleDiode system as a cost-effective more robust transfer standard and the TeleYAG system as a prospective novel primary standard.

The TeleDiode system was realised using commercially available fibre optics in the telecom band which resulted in a compact and transportable device, with the potential for commercialisation. In the field, standard deviations of 3  $\mu\text{m}$  (i.e. a relative standard deviation of  $3 \times 10^{-9}$ ) over 800 m and 24  $\mu\text{m}$  over 4.7 km were successfully demonstrated.

The TeleYAG system was based on a highly specialised optical design. Two-colour inline refractivity compensation was achieved with this system. Combined measurement uncertainties between 0.2 and 0.6 mm were successfully demonstrated for distances up to 864 m in outdoor conditions. No additional environmental monitoring systems were needed. Traceability to the SI definition of the metre is directly implemented in the system design and makes the TeleYAG system a suitable primary length standard for distances over several hundred metres.

As well as the index of refractivity, air turbulence also affects optical long-distance measurements. Therefore, an optical turbulence meter was developed by the project to assess this effect in typical outdoor conditions. Initial results have indicated that for moderate turbulence conditions (e.g. wind speeds up to 3 m/s) standard deviations of 10  $\mu\text{m}$  for 80 m are possible, suggesting a fundamental limit for length measurements in the order of  $1 \times 10^{-7}$ .

In conclusion, the project reduced the achievable measurement uncertainty over 1 km from 1 mm under optimum conditions to 0.2 to 0.6 mm under reasonable conditions, i.e. for a moderate temperature window of 10 to 30°C due to limitations of the hardware used and wind speeds below approx. 3 m/s for acceptable turbulence levels. These standards have increased the reliability of the traceability chain in surveying.

### 2. Uncertainty of GNSS-based distance metrology, targeting absolute uncertainties of 1 mm or better

GNSS-based distance metrology is used ubiquitously. While its flexibility is an advantage of this technology, it suffers from uncertainty influences such as signal delays due to the signal traversing the troposphere and ionosphere, and satellite obstruction or signal distortions such as multiple reflections due to the vicinity of the receiver antenna. These influences are impossible to control and difficult to quantify. Therefore, to derive recommendations for optimum measurement strategies and for a sound measurement uncertainty assessment, individual uncertainty contributions were studied and isolated (as far as possible).

Fibre optics were used to synchronise the receiver clocks of two GNSS receivers and this 'common clock' approach eliminated the need to determine the clock as a free parameter. Thus, an unperturbed access to other parameters should have been theoretically possible but, in practice, the receiver electronics were very sensitive to the local environment and this could not be eliminated. Nevertheless, the project successfully demonstrated that the fibre optic approach enabled high resolution height measurements which is important for the monitoring of critical buildings such as bridges.

In addition to this, the optimum processing strategy for the linked parameters height, receiver clock and tropospheric delay was investigated using the standard GNSS analysis approach. With this, a correction strategy was successfully applied to co-located GNSS stations reducing height discrepancies from the centimeter-level to the millimeter-level.

The importance of symmetry in the measurement set up was underlined through outdoor studies on the effect of mounting GNSS antennas on geodetic pillars and studies of typical obstruction scenarios. In the case of symmetrical set ups (same antenna types and mounting, in a similar environment), absolute and standard deviations below 0.5 mm could be achieved, even with additional obstructions. These unexpected results indicate that satellite obstruction itself does not substantially affect measurement uncertainty.

Finally, the project investigated a practical approach for the assessment of uncertainties in GNSS-based distance metrology. The results showed that deviations from reference coordinates taking into account the uncertainty of these reference coordinates and the observed standard deviation were a good indication of the achievable measurement uncertainty for specific configurations and measurement times.

In conclusion, although, a general method for millimetre uncertainties in GNSS could not be produced, the project improved the quantification of relevant uncertainty contributions, and suggested improvements for reducing measurement uncertainties in GNSS-based distance metrology.

### 3. Femtosecond laser-based many-wavelength interferometry for long-distance metrology

Since their invention in the last decade, optical frequency fibre combs have been advocated as ideal sources for high accuracy length measurements. They provide multiple laser modes with frequencies that can be directly locked to reference clocks in the radio frequency regime, and thus directly to the SI definition of the metre. However, prior to this project, commercially available fibre combs were characterised by low repetition frequencies which complicated their use for length metrology applications. Therefore, the project studied several approaches to address this, such as mode filtering by air-spaced or fibre based Fabry-Perot cavities. From the results a design for a novel broad band dual-comb generator was produced which can be used as a potential source for length metrology applications, as well as being applied to spectroscopic applications.

Heterodyne multi-wavelength interferometry as a fast detection technology was also investigated by the project. It was successfully used to demonstrate a relative measurement uncertainty of  $5.3 \times 10^{-7}$  (0.53 mm) for a measurement distance of 20 m, for cavity-enhanced electro-optic frequency combs.

In conclusion, in terms of length measurement, spectral interferometry proved to be the most successful method with deviations from a counting interferometer below 1  $\mu\text{m}$  up to 50 m, corresponding to a relative measurement uncertainty of  $2 \times 10^{-8}$ . This is the first time that spectral interferometry has been successfully applied over such distances.

### 4. Improvement of state-of-the-art surveying practice with respect to length metrology

One of the major outcomes of the project was the linking of three European primary geodetic baselines in Finland and Germany via an extensive field study using different transfer standards such as the TeleYAG and TeleDiode systems developed in objective 1, as well as commercial state-of-the-art devices. Following their comparison, these primary geodetic baselines can now provide European surveyors with SI traceable calibration of their devices with low uncertainty.

The project also developed the sophisticated “Revolver” field test for the validity of GNSS antenna calibration parameters. This test is based on measurement campaigns with multiple antennas. By suitable antenna swapping and rotating, and using high-level analysis, the test procedure is sensitive to 0.1 mm level for the absolute residual offsets of each antenna for the North and East component and relative residual offsets for the ‘Up’ component. Therefore, a verified tool to test GNSS equipment in the field with reduced instrumentation is now available for European surveyors.

Finally, two good practice guides were produced by the project with the aim of reducing uncertainty contributions in GNSS-based distance metrology and in electronic distance meters baseline calibrations. These good practice guides are available for end-users on the project’s website <http://www.emrp-surveying.eu/emrp/2984.html>.

In conclusion, the project was able to improve the metrological core of European surveying and to provide measurement and verification strategies for daily work in surveying. These combined outputs contribute to improving the state of the art of surveying practice.

### 5. Local tie metrology for the Global Geodetic Observing System (GGOS)

Local tie vectors connect the reference points of different space-earth measurement observing systems. Their monitoring networks are highly complex, but are crucial for the generation of a global reference system which forms the basis for GPS-based navigation or global observations of climate-induced changes, for example. This project theoretically investigated existing networks and derived complex models for uncertainty propagation. Different approaches were used to estimate the overall achievable measurement uncertainty of contemporary local tie vector monitoring in the order of 1 – 2 mm. The project also installed GNSS-based and terrestrial real-time 3D observation systems at the geodetic fundamental stations of Onsala, Sweden and Metsähovi, Finland. The observation systems are capable of monitoring reference points during system operation in real-time. They can therefore directly measure unexpected position changes induced, for example, by temperature expansion. This is expected to reduce the uncertainty of local tie vectors, in the longer term and provides a promising ‘new’ approach.

In conclusion, the project established analysis tools to assess the measurement uncertainty of local tie measurements. This is necessary to make quantifiable advances in the measurement technology. The 3D observation systems installed in the project will be studied in the community in the next few years. The goal of 0.1 mm, as inspired by geodetic roadmap papers needs further work and will require a much larger effort from the surveying community in forthcoming years.

### **Actual and potential impact**

Traceability of long distance measurements in surveying remains a highly challenging field. This project developed scientific and technological solutions for high-accuracy long distance metrology. Lower uncertainty levels were successfully met by the project, including reducing the measurement uncertainty of optical distance measurements in air well below 1 mm over a distance of 1 km. Many of these outputs are already available to end users to improve traceability in surveying, geodesy and earth sciences.

### *Dissemination activities and stakeholder engagement*

35 publications were published, predominantly in high impact journals such as Scientific Reports, Optics Letters, Journal of Applied Geodesy, Review of Scientific Instruments and Measurement Science and Technology. The publications as well as many presentations are available for end-users on the project website [www.emrp-surveying.eu](http://www.emrp-surveying.eu).

A stakeholder advisory board with representatives from surveying, device manufacturers, space geodesy and high energy physics regularly monitored the project and provided feedback.

Presentations were given at more than 40 conferences, such as at the International Association of Geodesy Scientific Assembly, the International Earth Rotation and Reference Systems Service Workshops and MacroScale. Furthermore, the project was invited to present its work on local tie metrology at the International

Very Long Baseline Interferometry Service General Meeting in South Africa, and the project coordinator was invited to present the outcomes of the project to the association of professional surveyors in Germany, the "Deutscher Verein für Vermessungswesen (DVW)".

25 presentations were given by the consortium and external researchers at the "1st Workshop on Metrology for Long Distance Surveying", attended by 50 worldwide experts and end-users. The 3rd Joint International Symposium on Deformation Monitoring jointly organised by the International Federation of Surveyors and the international association of geodesy also hosted 2 dedicated sessions for the presentation of the project's results.

### *Contribution to standards*

The consortium discussed its outcomes with several major standardisation bodies, including the ISO/TC 172/SC6 "Optics and photonics - geodetic and surveying instruments" and DIN NA 005-03-04 AA "Geodätische Instrumente und Geräte (SpA zu ISO/TC 172/SC6)" (the German standardisation equivalent committee to ISO/TC 172/SC6). The project's GNSS work (objective 2) was presented to both committees.

Two Good Practice Guides (objective 4) were published:

1. Good practice guide for the calibration of EDMs on baselines
2. Good practice guide for the calibration of GNSS-based distance meters under different conditions

The project, developed close collaborations with standardisation bodies in local tie metrology. A member of the consortium was elected head of the International Earth Rotation and Reference Systems Service (IERS) Working Group on Site Survey and Co-location and the conclusions from the project's local tie studies (objective 5) were fed into the development of a best practice guide for core sites (geodetic fundamental stations) in the GGOS [http://cddis.gsfc.nasa.gov/docs/2015/SiteRecDoc\\_Rev2\\_D3.4.pdf](http://cddis.gsfc.nasa.gov/docs/2015/SiteRecDoc_Rev2_D3.4.pdf)

### *Early impact on traceability in surveying and geodesy*

Project outcomes are being taken up by several organisations:

- Discussions are underway with a French SME about the commercialisation of the one wavelength TeleDiode system (from objective 1) for high-end long distance measurements.
- The use of optical cavities combined with mode-locked femtosecond lasers (objective 3) for the length characterisation of piezoelectric actuators is being discussed with the Czech company MESING who specialise in the design and manufacture of length measuring devices for the engineering industry.
- A specialised software tool developed in the project for the analysis of the data from the comparison of the three European primary geodetic baselines (objective 4) will be made available to the surveying community.
- PTB will use the data from the comparison from objective 4, to establish a Calibration and Measurement Capability (CMC) service for the long-distance calibration of EDMs.
- CNAM will make the TeleDiode prototype (from objective 1) available to the French national geodesy and cartography institute IGN for use in a practical survey in order to demonstrate the TeleDiode prototype's accuracy and productivity. Joint studies between CNAM and IGN are currently on-going.
- CNAM has developed an all-fibred EDM with surprisingly high performance at low cost. This is expected to be available within the next year.
- The 3D real time local tie monitoring system (from objective 5) will be permanently installed and used at the geodetic fundamental stations of Onsala, Sweden, and Metsähovi, Finland. It will contribute to the International Terrestrial Reference Frame (ITRF), a set of coordinates located on the Earth's surface.
- At Metsähovi, the project's sophisticated "Revolver" test field (objective 4) was integrated into the local tie network and is now routinely used there to check antennae deployed for local tie monitoring of the ITRF.

### *Potential impact*

The project's outcomes will help surveyors and researchers in geosciences face the challenge of measuring distances over several hundred metres up to kilometres with lower uncertainties. The potential fields of application are landslide monitoring, the monitoring of critical sites like future carbon dioxide or nuclear waste repositories, and for ensuring the accurate positioning of agricultural machinery such as combine harvesters and thus helping to control European agricultural subsidies.

The results of the GNSS studies have triggered further studies at PTB regarding the optimum set up of the GNSS system for time transfer. These studies may lead to a refurbishment and optimisation of this important installation in the future.

PTB intends to improve transportability of TeleYAG technology further to offer calibration service of primary baselines for legal metrology purposes in legal metrology.

Scientific conclusions on local tie metrology will influence local tie monitoring at geodetic fundamental stations of the GGOS in future.

## 2 Project context, rationale and objectives

Distance measurement in one dimension (1 D) is a fundamental and well-advanced measurement technology in many disciplines. For 1D distance measurements, surveying and geodesy can use sophisticated and commercially available measurement tools based on two fundamental technologies: (I) either a direct optical distance measurement based on the propagation velocity of light or (II) the analysis of signals received from global navigation satellite systems (GNSS). By combining either of these technologies with advanced analysis methods typically used in the field, surveyors are capable of astonishing accuracy, in cadastral work (i.e. the establishment and re-establishment of real property boundaries), industrial metrology, or in hazard monitoring.

However, in terms of surveyor's or geoscientist's most critical tasks for society i.e. the prediction of landslides, subsidence, or sinkholes at an early stage, i.e. movements of 1 mm per year (R02), they face the challenge of measuring distances over several hundreds of metres up to kilometres with uncertainties at the millimetre level and from these measurements having to determine conclusive evidence for millimetre changes per year from data sets taken over decades (R01). Changes in the order of 0.2 mm per year are a typical magnitude when monitoring crustal deformations in the vicinity of locations of nuclear power plants (R03) and similar measurements are needed in the context of motion observation of micro-tectonic plates (R04) or in studies of the Greenland ice sheet (R05) and postglacial rebound phenomena (R06). Therefore, for the long-term comparability of results and monitoring of such hazards, traceability to the SI definition of the metre is essential as well as a substantial improvement of the level of measurement uncertainty to the sub-millimetre level.

Another challenge for surveying technology is the projection of positions and coordinates to sub surface levels where GNSS position sensors cannot be operated. One prominent example of the current limitations of this was the determination of the baseline distance for the time of flight neutrino experiment between CERN and the OPERA detector in the Gran Sasso underground laboratory. The overall uncertainty of 20 cm of the 730 km baseline distance measurement was wholly determined by an electronic distance meter (EDM) measurement of the last kilometre which was performed in a tunnel (R07). Uncertainties in the order of decimetres are also a growing problem in the mining sector and here the question arises "how to relate underground operations [...] to the surface" (R08). The refractivity compensated EDM approaches developed in this project were able to deal with the complicated ambient conditions underground and thus the current relative uncertainty of  $10^{-5}$  (R07) for these kinds of measurements can now be reduced by at least one order of magnitude.

Even in cadastral work, which is most common in densely populated urban areas, the current demands for measurement accuracies are so high, that legal measurements of coordinates, requires traceability with an uncertainty at the (sub-)centimetre level.

Science is also challenging the accuracy of state-of-the-art surveying technology, for example, progress in high energy physics requires ever larger particle accelerators, combined with an increased need for accurate positioning, and the realisation of the Compact Linear Collider (CLIC), e.g., an envisioned linear accelerator of 50 km length, the CERN large scale metrology group expects length measurements with an uncertainty of 1 mm. Further to this, the next generation of atomic clocks with uncertainty in the  $10^{-18}$  range will require knowledge of their height above the geoid with centimetre accuracy in order to allow meaningful comparisons and time and frequency dissemination (cf. refs. (R09) and (R10)). Currently the clock's height is based on levelling with respect to national height references combined with models of the geoid undulation, or alternatively, the clock's ellipsoidal height can be determined by GNSS. However, preliminary studies have shown significant discrepancies in the orders of several centimetres in both approaches, and therefore a better understanding of the calibration and uncertainties of GNSS determined height coordinates (given in metre) is needed.

Immediate impact on long distance measurement uncertainty could be made by tackling the major source of uncertainty of the two fundamental technologies: optical and GNSS based measurement technologies: i.e. the uncontrollable environment effects on the measurand electromagnetic waves, and on the measurement equipment exposed to the environment. In the case of optical methods, further knowledge is needed on the index of refraction in order to reduce measurement uncertainty. Intrinsic optical compensation could be used to reduce the measurement uncertainty by one order of magnitude, for example by creating novel primary standards for the calibration of reference lengths. However, in order to achieve the required sub-millimetre measurement uncertainties for distances over several hundred metres, the impact of turbulence when applying such optical methods must also be addressed.

In the case of GNSS, a number of effects influence the measurement uncertainty at the millimetre level, such as the propagation of the signals through the troposphere and ionosphere, or the deflection of the signals by

the local surroundings, which leads to so-called ‘multi-path effects’. Therefore, better and more robust quantification would help to derive optimum measurement strategies and smaller measurement uncertainties.

In the case of optical measurement technologies novel methods like optical frequency combs (i.e. femtosecond laser-based many-wavelength interferometry) have the potential to be used for more accurate solutions for length measurement. During the last few years several measurement schemes for distance measurement with a femtosecond frequency comb have been developed and demonstrated and one such promising approach is based on the exploitation of the individual modes (all having different wavelengths) that are present in a femtosecond comb. Many-wavelength interferometry with thousands of wavelengths had been demonstrated for short distances (< 1 m) prior to the start of this project (R11). The main advantage of the many-wavelength approach is that it provides sub-wavelength accuracy in combination with a large range of non-ambiguity. Furthermore, the long coherence length of these sources enables interferometry over very long distances (in principle up to thousands of kilometres). These properties are valuable for long-range applications, like in surveying, or for space applications (e.g. distance determination between satellites), but for this to be really achieved, new measurement concepts need to be investigated and tested outside of the laboratory environment.

Further to this, space geodetic observations are highly critical for earth science observations and for the maintenance of the global and local GNSS reference system. Geodetic reference networks are sustained by processing the information of various observation techniques including, for example, GNSS reception, Satellite Laser Ranging (SLR), Very Long Baseline Interferometry (VLBI), or gravimetric measurements. These observations are simultaneously performed and presently combined at fifteen geodetic fundamental stations across the world, forming the backbone of the Global Geodetic Observing System (GGOS) (R12),(R13). The current requirement of  $\pm 1$  mm uncertainty for slope distances in 3 D for the relative positions of the respective reference points is not achievable without a proper calibration of all instruments and a traceable scale in the GNSS measurements. Therefore, on site, optical techniques, like EDM and levelling, and “short range” GPS need to be used to connect the respective reference point positions with so-called “local tie vectors”. However specific applications for positioning, e.g. in sea level monitoring for disaster prevention or climatologic studies demand an even lower uncertainty for positioning services in the near future (R14). Thus in order to improve measurement services in line with this, real-time capable 3D surveying methods are required to substantially improve the uncertainty of the determination of the spatial correlation of these measurements, i.e. the local tie vectors, together with appropriately optimised measurement strategies.

Finally, in order to improve surveying work in the field, it is important to offer good practice guidance for state-of-the-art surveying. This should include field-capable optical standards for long-distance baseline calibrations and revised guidelines for the calibration of both EDM and GNSS-based distance meters.

### **Scientific and technical objectives**

The project united metrologists, surveyors and geodesists in the need to improve long-distance metrology. The scientific and technical objectives of the project were:

6. To improve optical measurements in air. In particular, the inline compensation of the refractive index along the whole beam path, and the impact of turbulences on the measurement, with a target relative uncertainty of  $10^{-7}$  over a distance of 1 km.
7. To gain a better understanding of the uncertainty of GNSS-based distance metrology. This will allow the development of a sound uncertainty model and an optimised field calibration procedure, targeting absolute uncertainties of 1 mm or better.
8. New concepts for the application of femtosecond laser-based many-wavelength interferometry to long-distance metrology with a targeted relative measurement uncertainty significantly better than  $4 \times 10^{-7}$  under controlled environments.
9. To develop solutions to improve state-of-the-art surveying practice, ranging from field-capable optical standards with relative uncertainties of  $10^{-7}$  for long-distance baseline calibrations, over refined guidelines for the calibration of both EDM and GNSS-based distance meters, up to an extensive inter-comparison of major primary geodetic baselines in Europe.
10. To investigate different approaches to real-time monitoring of local ties at geodetic fundamental stations, both experimentally and theoretically. Thus, fundamental metrology for the Global Geodetic Observing System (GGOS) will be developed with an overall target to reduce the uncertainty of reference frames to 0.1 mm.

### 3 Research results

#### 3.1 The optical distance measurement in air

In case of optical measurements in surveying, the achievable measurement uncertainty is limited by the fact that the medium i.e. air changes the speed of light, and thus, the scale used. In practice, this limits the achievable relative accuracy of state-of-the-art distance meters to  $10^{-6}$  and therefore the project pursued as its objective 1

*“To improve optical measurements in air. In particular, the inline compensation of the refractive index along the whole beam path, and the impact of turbulences on the measurement, with a target relative uncertainty of  $10^{-7}$  over a distance of 1 km.”*

There were several scientific and technological routes possible for the project to use in order to achieve the overall target of a relative measurement uncertainty of  $10^{-7}$  over a distance of 1 km. The project chose three different approaches based on refractivity compensation:

1. the highly accurate interferometric TeleYAG system,
2. the more robust and easier-to-use TeleDiode system, and
3. a spectroscopic thermometer.

This resulted in 3 different solutions with different applications. The impact of turbulence was also quantitatively studied by the project.

##### 3.1.1 The TeleYAG system as novel primary standard for baseline calibrations

The TeleYAG system realises an absolute distance measurement (ADM) with in situ compensation of the refractive index of air for the primary realisation of the SI definition of the metre over distances of up to approximately one kilometre. It is based on heterodyne multi-wavelength interferometry, both for the distance measurement itself and the dispersion-based refractivity compensation.

One challenge for such an approach is the development of a stable and suitable radiation source. A frequency doubled Nd:YAG (wavelengths 1064 nm and 532 nm) laser was stabilised onto a second laser with a frequency difference of 20 GHz at 1064 nm, leading to beat frequencies between them of 20 GHz at 1064 nm and 40 GHz at 532 nm. These beat frequencies generated the “synthetic wavelengths” of  $\approx 15$  mm at 1064 nm and  $\approx 7.5$  mm at 532 nm which were used as the length scales for the absolute distance measurement. Since the unambiguous measuring range is half of the synthetic wavelength, additional longer wavelengths were generated with acousto-optic frequency shifters. The simultaneous measurement of the optical path with the wavelengths at 1064 nm and 532 nm leads to different results due to the dispersion in air which can be used to compensate the refractive index (R01).

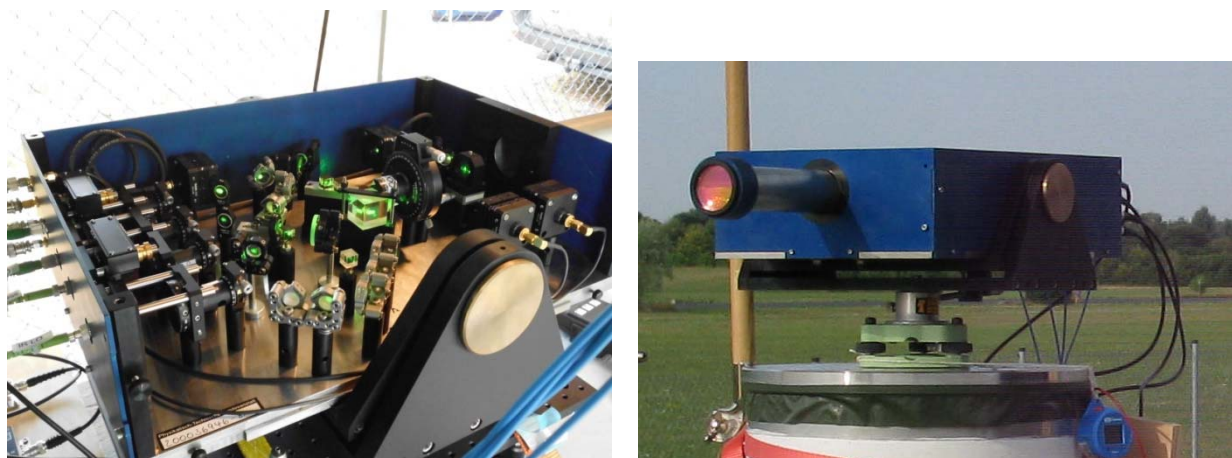


**Figure 1.** Results at the Munich baseline with the instrument on pillar 0 m (left) and on Pillar 18 m (right).

The interferometer as shown in Figure 1 works with the heterodyne detection of the signals. Four photo detectors for a reference and a measurement path and both wavelengths receive the signals of both lasers at different heterodyne frequencies (5 MHz and 7 MHz) simultaneously (R16). The signal phases are evaluated by field programmable gate arrays (FPGAs) connected with analogue to digital converters.

A major challenge of this measurement scheme is a very unfavourable scaling of measurement uncertainties. For a measurement with a synthetic wavelength the uncertainties are scaled by the ratio of synthetic to optical wavelength, i.e. a factor of approx. 14000. In addition, the dispersion-based refractive index compensation enhances uncertainties by an additional factor of 21.5. Therefore, in total, any uncertainty of the primary measurements is scaled by a factor of 300 000 in the final result.

Consequently, the optimisation of the TeleYAG system required a large amount of effort from the project. The TeleYAG system was first verified against a counting Helium-Neon (HeNe) laser interferometer at the 50 m comparator (geodetic base) of project partner PTB (R16). However, problems with the fibre collimation lead to linear deviations in the measured length and thus the mechanical design of the fibre collimation was changed before outdoor measurements on baselines were performed. First measurements on the 600 m PTB baseline and on the 1 km baseline of the University of Neubiberg, Germany, revealed a severe instability of the length offset of the device which could not be explained by mechanical reasons. The deviations between the individual 1064 nm and 532 nm results were up to 0.5 mm. The weather conditions were extreme with temperatures up to 36 °C. Figure 2 shows two result sets on the 1100 m baseline. The large deviations of up to more than 1 mm can be explained by the extreme temperature and the instability of the offset. The instability, however, prevented the evaluation of the refractive index compensated results.

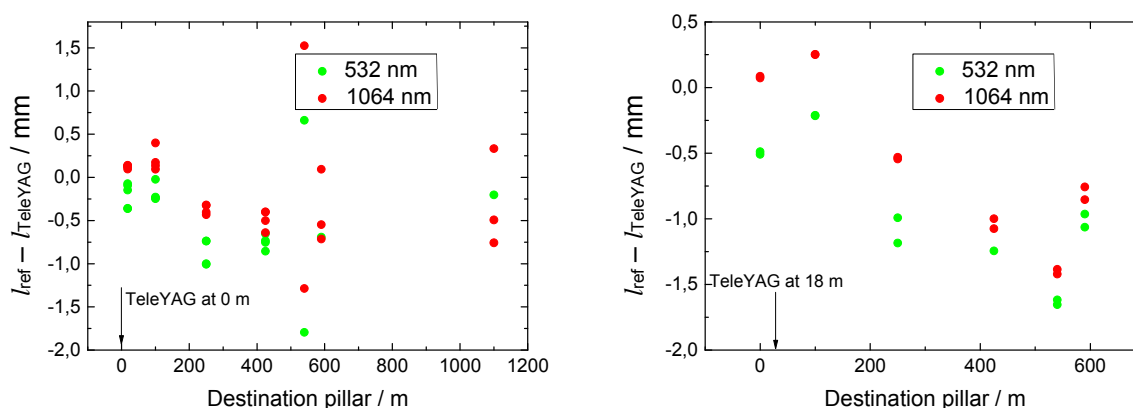


**Figure 2.** Results at the Munich baseline with the instrument on pillar 0 m (left) and on pillar 18 m (right). Reference lengths  $l_{ref}$  were determined by scale transfer by the Finnish Geodetic Institute.

For the final campaign at the Nummela standard baseline in Finland the TeleYAG system interferometer was optimised for an easier alignment. More importantly, the measurement strategy was adjusted for coping with the unresolved offset instability. The TeleYAG was mounted on the telescope pillar in front of a pillar 0 m and stayed fixed for the whole week. The reflector was placed on pillar 0 m and the offset was measured. After that the reflector was moved to the target pillar and the offset was subtracted from the measured length. This “differential absolute” measurement approach compensated to first order the instability of the offset well. As a consequence, the refractive index compensated results could be calculated. In the left graph of Figure 3 the results for both wavelengths with the calculated refractive index from temperature, pressure and humidity sensor data are plotted. The difference from the reference values remains below 0.55 mm for each single data point. With the exception of one systematic outlier, the mean values are nicely consistent with the reference value derived from white light interferometry. The refractive index compensated results in the right graph of figure 3 have some outliers above 1 mm caused by the remaining offset instability during a measurement. However, although the standard deviation increases due to the uncertainty scaling, the mean value agrees again well with the reference values. For the latter analysis, only a humidity sensor contributed as external sensor.

It should be noted that the standard deviation of the refractive index compensated result is length independent and smaller than 50  $\mu\text{m}$  for 10 s averaging time, corresponding to  $50 \mu\text{m}/300000 = 0.17 \text{ nm}$  for the

combination of the four optical wavelengths which is a remarkable performance for an outdoor measurement. The experimental results and the theoretical analysis indicate that a combined measurement uncertainty for the refractivity compensating result well below  $5 \times 10^{-7}$  over a kilometre is feasible. This is supported by results from the EMRP JRP IND53 LUMINAR (R17).

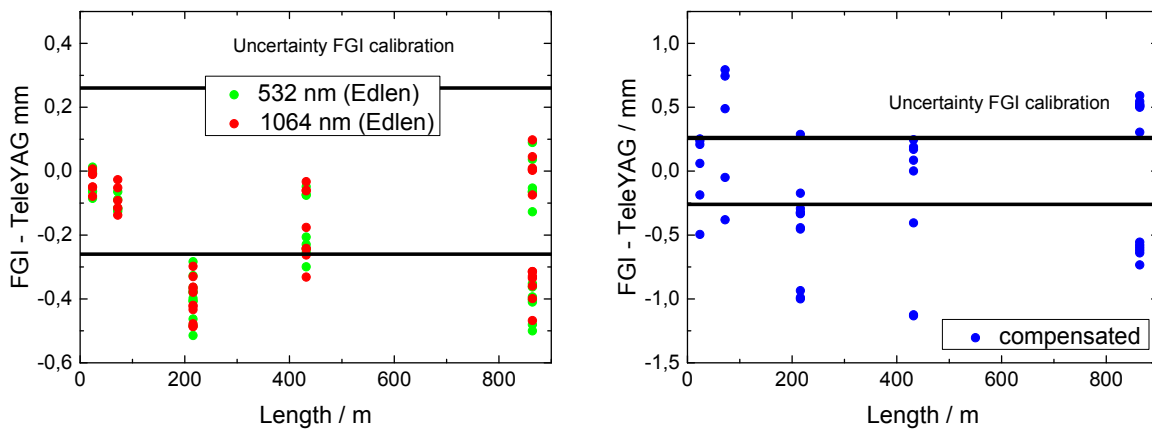


**Figure 3.** Results at the Nummela standard baseline evaluated with the sensor data (left) and the refractive index compensated results (right).

### 3.1.2 The TeleDiode System as novel transfer standard

The TeleDiode system is a transportable device for transferring the scale from a reference baseline to other baselines. The system design was based on optical fibre technology and operates simultaneously at 1550 nm and 785 nm. This dual wavelength operation enables the measurement of the distance without measuring temperature and air pressure, which are the most limiting parameters in long distance measurement in air. The TeleDiode system is easily transportable and composed of a measurement head (as shown in Figure 4) and a control unit ("6U" rack).



**Figure 4.** Photograph of the complete TeleDiode system in operation at the Nummela baseline (left) and a CAD view of the optical head (right)

The TeleDiode system's 1550 nm port turned out to have performances as good as expected: 2-3  $\mu\text{m}$  of resolution for 10 ms of integration with an accuracy better than 10  $\mu\text{m}$  over 50 m. At 785 nm the TeleDiode system's performances were 7-8 times less accurate than at 1550 nm. This prevented using the TeleDiode system in its current state as an efficient air index compensated telemeter. Nevertheless, the use of the 1550 nm telemeter enabled the transfer of kilometric reference baseline's scale at 300  $\mu\text{m}$  level, as long as the temperature along the baseline could be determined with 0.3  $^{\circ}\text{C}$  accuracy.

Reasons for the failure to obtain sufficient resolution and accuracy at 785 nm were identified and attributed to firstly the optical amplification technique of the reflected signal before detection and secondly to residual optical feedback due to fibre connections. Unfortunately, these two issues could not be improved within the lifetime of the project.

The most impressive result with the TeleDiode system is probably the high resolution of the telemeter: when atmospheric conditions are sufficiently favourable to avoid beam wandering or large effective index variations, the project obtained at 1550 nm a resolution of 3  $\mu\text{m}$  over 864 m (corresponding to  $3 \times 10^{-9}$  in relative value) in real time measurement. Figure 5 illustrates this result.

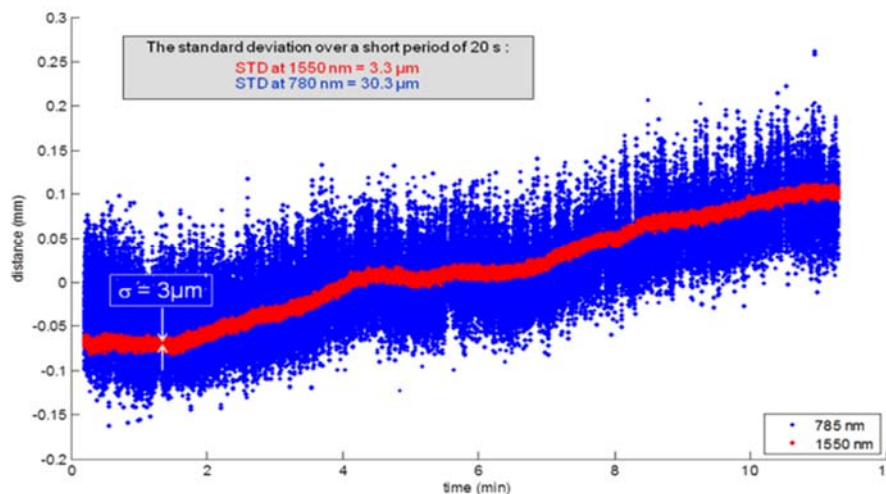


**Figure 5.** Raw data obtained over 864 at both wavelength, with a short term sigma of 3  $\mu\text{m}$ .

In addition, a successful comparison with a reference baseline (864 m at Nummela, Finland) was performed using the TeleDiode system. The result is depicted in figure 6. The main uncertainty component of the comparison beyond 200 m was due to the determination of air temperature along the baseline, but it should be stressed that, the deviation from the reference value did not exceed 300  $\mu\text{m}$ .

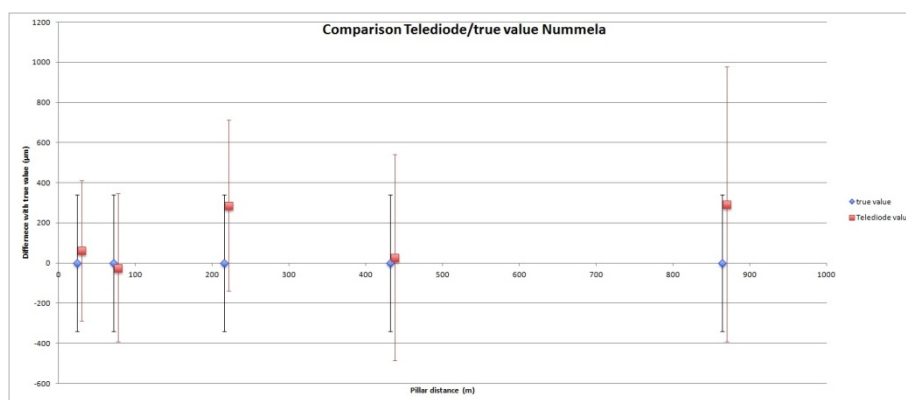


**Figure 6.** Comparison between reference value and Telediode measurements, uncertainty bars represent 2 sigma intervals

Optimisation work on the TeleDiode system is ongoing and the telemeter will be compacted to include all electronics on the optical head, which should lead to a reduction in cost. Air index compensation has still not been achieved at the sub-mm level but changing the two-wavelength laser system of the prototype should lead to significant improvements. Furthermore, the first outdoor tests over longer distances than 1 km are very encouraging to reach 5 – 10 km range with sub-mm accuracy with the same principle of operation.

Overall, its performance makes the TeleDiode system a very promising transfer standard for the traceable dissemination of the metre to kilometre distances.

### 3.1.3 Air index investigations by long distance spectroscopic thermometry

The sensitivity of electronic distance meters (EDMs) to temperature can be reduced significantly by measuring at two or even three wavelengths. However, the disadvantage of this is added complexity and increased sensitivity to humidity. Therefore, an alternative is to measure the effective temperature along the beam spectroscopically, in effect realising a spatially continuous temperature sensor network. Air thermometry based on oxygen spectroscopy for air refractive index compensation was developed in the EURAMET iMERA-Plus 2008-2010 project “Absolute long distance measurement in air” and one of the objectives of the present work was to extend the measurement range up to 1 km with a targeted measurement uncertainty of 100 mK, corresponding to a relative uncertainty in distance of  $10^{-7}$ . To achieve this, simulations of air absorption were carried out in order to find the most suitable absorption lines and to determine the best measurement procedure. Typically, spectroscopic thermometry is performed by measuring the ratio of two absorption lines as this eliminates the signal dependency on concentration variations. But finding two well-isolated absorption lines with suitable temperature dependencies and line strengths turned out to be difficult for the project, as the oxygen concentration in the atmosphere is extremely constant (R18) and as a consequence, it was not necessary to determine the line strength ratio of two absorption lines in order to get rid of the concentration dependency. This simplified the setup so that the amount of oxygen (number density) in the air can be determined to sufficient accuracy from the atmospheric pressure using the ideal gas law and the known concentration with corrections for water vapour and CO<sub>2</sub>.

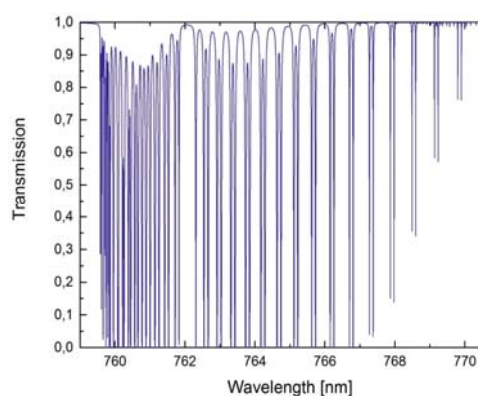


**Figure 7.** Simulated atmospheric transmission over 1 km. All absorption lines seen here are due to oxygen.

Based on simulations using line parameters from the HITRAN database, it was decided that a magnetic dipole transition at 769.23 nm ( $13000.0 \text{ cm}^{-1}$ ) in oxygen was the most suitable choice: as there are no nearby transitions interfering with the line area determination, the line strength is relatively sensitive to temperature variations (around 2 %/K), and single-mode distributed-feedback semiconductor lasers are readily available. Fig. 7 shows the expected atmospheric transmission over 1 km around 765 nm. In particular on the long-wavelength-side there are several well-isolated absorption lines, and the one to choose depends predominantly on the target distance.

For measurements at the Nummela 864 m standard baseline, a simple setup based on a single, modulated distributed feedback (DFB) diode laser was built. The diode laser was scanned over the chosen transition with a frequency of 1 Hz as the output power was chopped by an electro-optic intensity modulator at 10 kHz. The output of the laser was split three ways: (1) to a reference photodiode, (2) to a temperature-stabilised fibre etalon for calibration of the frequency scan and (3) to the actual spectroscopy beam. The spectroscopy beam was collimated with a 4” aspheric lens and sent along the Nummela baseline, where at the far end an inexpensive 8” collector lens focused the beam onto a large-area photo receiver. The signal was then amplified and sent along twisted and shielded pair-cable back to the transmitting end where two lock-in amplifiers and a PC were used to record the signals. Figure 8 shows an example of a very clean absorption signal that can be obtained in calm weather over a distance of 864 m.

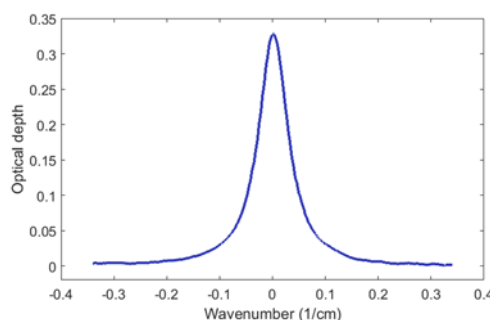


**Figure 8.** Oxygen absorption at  $13000.0 \text{ cm}^{-1}$  (769.23 nm) in excellent conditions over a distance of 864 m.

An area-normalised line profile was then fit to the absorption line using robust algorithms, and the scaling factor required was then used to determine the line area. From the measured pressure and humidity, and from the known O<sub>2</sub> concentration, the temperature could be determined (R19). But in practice, a calibration of the line intensity was needed. Figure 9 shows the spectroscopic temperature (blue) versus the average (red) and minimum-maximum (pink) temperature given by 4 Pt-100 sensors placed along the 864-m Nummela baseline. Overall, during the four-day-long test campaign, the two techniques (i.e. spectroscopic versus electronic thermometry) agreed to within 500 mK. Part of the deviation can be attributed to the imperfect capture of the effective temperature by the reference sensor network, nevertheless these results are encouraging and support the further development of this spectroscopic thermometry.

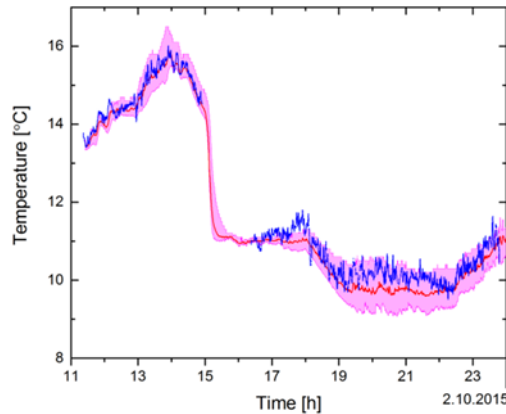


Figure 9: Spectroscopic versus electronic thermometry at the Nummela 864-m baseline.

### 3.1.4 Turbulence and optical distance measurement

It is well known that, aside from the propagation speed, the propagation path of a laser beam in air is affected by temperature gradients. Indeed, if one performs optical measurements outdoors with a laser beam parallel to the ground, you will observe a vertical displacement of the beam because of the vertical temperature gradient caused by the sun's heating. In particular, during daytime higher layers of air are warmer than layers closer to the ground. This temperature gradient causes a gradient of the air refractive index which yields a downwards bending and the opposite happens in night time with the beam bending upwards.

From a mathematical point of view, a vertical gradient of refractive index,  $dn/dz$ , causes a deflection of a laser beam with a refractive angle  $\delta$  equal to

$$\delta = \frac{1}{R} \int_0^R \frac{1}{n} \frac{dn}{dz} (r - R) dr \quad [1]$$

where  $R$  is the beam propagation length. In case of constant gradient, equation [1] becomes

$$\delta = -\frac{1}{2n} \frac{dn}{dz} R = -\frac{1}{2n} \frac{dn}{dT} \frac{dT}{dz} R \quad [2]$$

Hence, the refractive angle is proportional to vertical temperature gradient and to the beam propagation length. According to equation [2], a gradient of 0.5 °C/m causes a refractive angle of 4" for a path length equal to 78 m, in agreement with the experimental results obtained. As a consequence, the beam bending due to a vertical gradient of refractive index causes a beam displacement according to the following equation

$$d = -\frac{1}{2n} \frac{dn}{dz} R^2 \quad [3]$$

This displacement can be important for long distance measurements even in case of small temperature gradients: for example, a gradient as small as 0.1 °C/m causes a beam displacement of more than 2 mm at a distance of 200 m.

The structure parameter of refractive index is used to distinguish between different turbulent regimes. For example, for  $C_n^2$  values smaller than  $8 \times 10^{-15} \text{ m}^{-2/3}$  the turbulence is weak, while for  $C_n^2$  values greater than  $10^{-13} \text{ m}^{-2/3}$  it is considered as strong turbulence. In the special case of horizontal propagation of a plane wave

on a distance  $L$ , there are some approximation formulas in the scientific literature that estimate optical parameters of interest from the knowledge of  $C_n^2$ , such as the beam wandering for a Gaussian beam, the phase variance or the intensity fluctuations. Another example, in the case of a laser with wavelength  $\lambda = 1 \mu\text{m}$ , an intense turbulence ( $C_n^2 = 10^{-13} \text{ m}^{-2/3}$ ) will cause a phase standard deviation of about 0.45 rad at 300 m.

There are different techniques to measure the structure parameter of refractive index and project partner INRIM chose to determine the structure constant of the refractive index  $C_n^2$  from the measurement of the variance of the angle of arrival of a laser beam  $\sigma_\alpha^2$  through the equation [4]

$$C_n^2 = \frac{p^2 \sigma_\alpha^2 a^{\frac{1}{3}}}{1.09 f^2 L} \quad [4]$$

where  $a$  is the diameter of the lens,  $L$  is the propagation path length,  $p$  is the pixel size,  $f$  is the focal length and  $\sigma_\alpha^2$  is the variance of the spot on the CCD. The set-up developed by INRIM for the measurement of the angle of arrival of a laser beam and its fluctuations due to temperature gradients and to turbulence, respectively, is shown in figure 10.

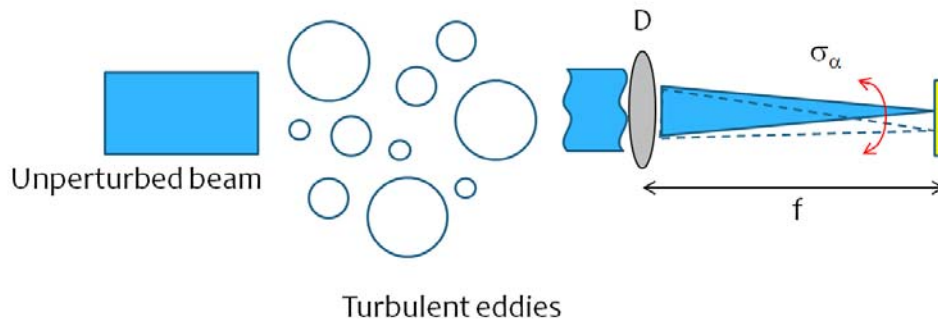


**Figure 10:** Scheme of the INRIM set-up to measure the angle of arrival of a laser beam and its fluctuations

Using the INRIM set-up, in summer the project obtained  $C_n^2$  values of about  $6 \times 10^{-13} \text{ m}^{-2/3}$  in sunny hours, when the sun's heating generates and feeds the air turbulence, and  $C_n^2$  values two order of magnitude smaller, i.e.  $5 \times 10^{-15} \text{ m}^{-2/3}$  in night time. Hence the INRIM set-up proved to be effective in distinguish between different turbulence domains.

In order to investigate the effect of turbulence on optical distance measurements, a synthetic wavelength interferometer was used to measure a distance  $d = 78 \text{ m}$  whilst the refractive index structure parameter was measured. As a result the project found a correlation between the standard deviation of the optical measurements and  $C_n^2$  of the order of  $10 \mu\text{m}$  for a distance of 80 m in the case of quite intense turbulent conditions (i.e.  $C_n^2 = 5 \times 10^{-13} \text{ m}^{-2/3}$ ). Moreover, there was a slight correlation between the standard deviation of the optical measurements and the wind magnitude.

Therefore, in order to reduce the effect of turbulence on optical distance measurement, it would be optimal to perform such measurements when the refractive index structure constant  $C_n^2$  is below  $10^{-13} \text{ m}^{-2/3}$  and wind speed below 3 m/s.

### 3.1.5 Conclusions

In surveying, optical measurements are typically performed under uncontrollable environmental conditions and therefore the accuracy of the measurement of these environmental quantities is limited. In practice, uncertainties below 1 K (kelvin) are only achievable under very stable conditions meaning that prior to the start of the project optical distance measurements were limited to a corresponding uncertainty of 1 mm (i.e.  $10^{-6}$ ) over 1 km distance.

This project developed optical methods suitable for use in the field that were capable of overcoming these limitations. One method used spectroscopy to build an optical thermometer, which was used to measure a temperature resolution below 300 mK over more than 800 m for averaging times of 120 s. The data can then be used to correct optical distance measurement data leading to uncertainties below 0.3 mm over this distance for the influence of the refractive index.

The project also developed devices for distance measurement in air that compensate for the index of refraction simultaneously with the distance measurement. The devices were based on an idea developed in the 1960s i.e. that if you measure a distance with two well-known optical frequencies and roughly determine the humidity, no further temperature or air pressure data is needed to derive the distance. The two devices were: the TeleDiode system as a cost-effective more robust transfer standard and the TeleYAG system as a prospective novel primary standard.

The TeleDiode system was realised using commercially available fibre optics in the telecom band which resulted in a compact and transportable device, with the potential for commercialisation. In the field, standard deviations of 3  $\mu\text{m}$  (i.e. a relative standard deviation of  $3 \times 10^{-9}$ ) over 800 m and 24  $\mu\text{m}$  over 4.7 km were successfully demonstrated.

The TeleYAG system was based on a highly specialised optical design. Two-colour inline refractivity compensation was achieved with this system. Combined measurement uncertainties between 0.2 and 0.6 mm were successfully demonstrated for distances up to 864 m in outdoor conditions. No additional environmental monitoring systems were needed. Traceability to the SI definition of the metre is directly implemented in the system design and makes the TeleYAG system a suitable primary length standard for distances over several hundred metres.

As well as the index of refraction, air turbulence also affects optical long-distance measurements. Therefore, an optical turbulence meter was developed by the project to assess this effect in typical outdoor conditions. Initial results have indicated that for moderate turbulence conditions (e.g. wind speeds up to 3 m/s) standard deviations of 10  $\mu\text{m}$  for 80 m are possible, suggesting a fundamental limit for length measurements in the order of  $1 \times 10^{-7}$ .

In conclusion, the project reduced the achievable measurement uncertainty over 1 km from 1 mm under optimum conditions to 0.2 to 0.6 mm under reasonable conditions, i.e. for a moderate temperature window of 10 to 30°C due to limitations of the hardware used and wind speeds below approx. 3 m/s for acceptable turbulence levels. These standards have increased the reliability of the traceability chain in surveying.

### 3.2 GNSS-based distance metrology

The second measurement technology used in long distance surveying is based on the reception of signals from GNSS and the correct interpretation of positions derived thereof. The whole system is highly complex, and the surveyor performing the actual measurement has very limited control of many parameters. The project's objective 2 was:

*“To gain a better understanding of the uncertainty of GNSS-based distance metrology. This will allow the development of a sound uncertainty model and an optimised field calibration procedure, targeting absolute uncertainties of 1 mm or better.”*

hence the project put a lot of emphasis on the investigation of uncertainty contributions since quantification at the level of one millimetre had been more heuristic rather than metrologically sound prior to the start of the project.

#### 3.2.1 GNSS based distance metrology using common clocks

The unresolved problem of GNSS-based distance metrology was tackled by the project using novel scientific tools in a joint interdisciplinary effort, both experimentally and theoretically, representing to some extent the merger of the disciplines that are abbreviated as Positioning, Navigation and Timing (PNT). A varying group of GNSS receivers were operated at the campus of PTB with antennas on different buildings, connected to the same hydrogen maser as a highly stable frequency reference. The frequency reference was transmitted through optical fibres to the different receivers, as schematically shown in Figure 11. This network was used as test-bed for the study of distance and distance variation determinations with the common-clock single-difference approach.

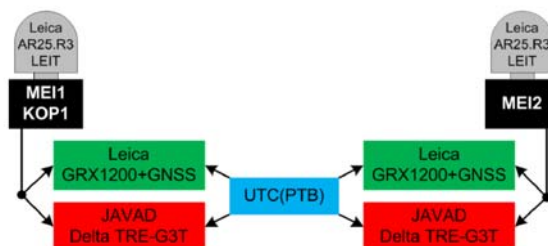


**Figure 11.** Measurement set-up for Common-Clock experiments, MEI1 and MEI2 represent two antenna locations on the same building, 5 m apart, whereas KOP1 was about 250 m apart on another building. Receivers of different brands were connected to identical antennas.

Even short distance measurements on the PTB campus showed, that several sources of disturbances exist which usually cancel each other out in more standard analysis based on double differences. Two state-of-the-art GNSS receivers of the same type in the same rack were also shown to exhibit different sensitivity to ambient temperature or humidity variations, exceeding the low picosecond range with time (R20). Thus, in contrast to prior expectations in the geodetic community, common-clock experiments unfortunately proved of little benefit for the investigation of second order uncertainty contributions for determining static distances. However, one has to note that the assumptions underlying the predictions by Santerre and Beutler (R22) which inspired this project's work could not be fulfilled in the project's installations or are likely to be fulfilled in an installation that comprises distributed equipment. However, common-clock set-ups that represent valuable and adequate test set-ups to investigate and compare the receiver performance of different manufacturers as well as to study various receiver related biases are of great interest for the international GNSS community especially the International GNSS Service (IGS).

In particular, it was shown that common-clock set-ups could be beneficial for kinematic analyses of distance changes between the GPS stations linked to a common clock (R23). To this end, the classical analysis method of GNSS baselines by using double differences (DD) can be replaced by single differences (SD) thanks to the common-clock set up that links the two receiver clocks at the baseline end points. In the common clock SD modelling approach, the clock stability requirement is mainly replaced by the link stability requirements, i.e. a clock with lower frequency stability can be used, provided that its signal is equally (at 1 mm accuracy) distributed to both receivers. Simulation studies were carried out by the project for the baseline between the

KOP1 and ME11 stations at PTB campus using the real satellite geometry. In one simulation run DD were formed, while in the second run SD were computed and a differential receiver clock error was estimated as a piecewise linear parameter. The clock modelling interval is varied from 15 minutes to 6 hours. The standard DD procedure is equal to an epoch wise estimation of the receiver clock, and can thus be used as a reference. A comparison of the different clock modelling intervals showed that clock modelling has almost no impact on the horizontal coordinate components. However, due to the significant correlation between height, receiver clock error and tropospheric delay, substantial improvements in the height component were shown: i.e. in case of clock modelling intervals of 15 minutes an improvement of 62% to the 1 mm level can be obtained. Thus the height component can be determined as precisely as the horizontal components.

An example dataset is shown in Figure 12. A kinematic coordinate time series was estimated by the project with both approaches with real data over the first 12 h of day-of-year (DOY) 297 in 2013. The differential receiver clock error was modelled as a piecewise linear function over 6 h. The data rate was 30 s and the cut-off angle 20°. A similar performance of both processing strategies could be observed for the North and East component with typical 1-2 cm variations of the kinematic coordinates. For the height time series, the impact of clock modelling is clearly visible and can be seen in Figure 12: where the coordinate time series (red) is much smoother. Here the root mean square (RMS) value is reduced from 2.4 cm (DD processing, blue) to 1.5 cm in case of common clock SD, thus, small high frequency variations in the height component can now be detected.

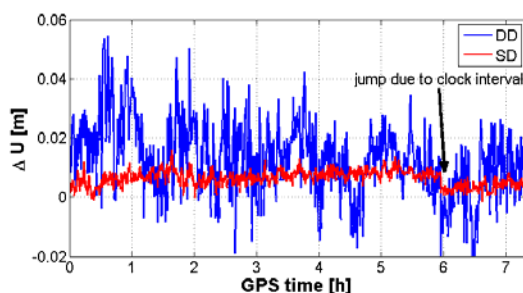


**Figure 12.** Comparison of kinematic Up coordinates for the 290 m baseline between Kopfermann and Meitner building. Blue: computed with standard DD, red computed with common clock single-differences.

### 3.2.2 Tropospheric influence and the combination of long and short baseline solutions

GNSS observations - both code and carrier phase - are one-way measurements yielding so-called “pseudoranges”. This is due to the fact that the transmitter time scale (e.g. GPS time) is not synchronised with the receiver time scale. For most applications this is not an issue since sufficient satellites are in view and a so-called receiver clock error is determined during the computation of positions to compensate the asynchronicity. However, strong correlations exist between the parameters; height; receiver clock; and tropospheric delay, sometimes called Bermuda triangle. Figure 13 shows the approximate relationship and how different effects are compensated by the parameters, e.g. a 1 mm error in the tropospheric delay yields a -3 mm error in height.

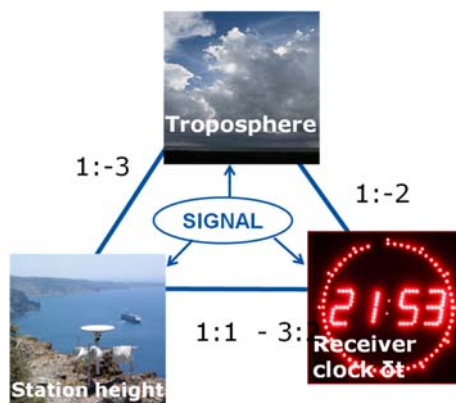


**Figure 13.** “Bermuda triangle” indicating the correlation between height - receiver clock error and tropospheric delay.

In the project an optimal processing strategy concerning the involved three parameters was developed to obtain maximum coordinate accuracy (R24). It was shown that best results could be obtained for a short baseline when identical observation conditions at both baseline endpoints exists, no tropospheric delay parameters were estimated, and double differences were computed that eliminate most of the remaining refraction effects. However, for combining short baselines (10 m – 1 km), like e.g., local ties at geodetic fundamental stations, with long baselines (> 50 km), the situation changes, as different analysis schemes yield optimal accuracy, i.e. for long baselines tropospheric parameters must be set up. Therefore as common analysis settings are normally used for all baselines in GNSS software packages, then this means that suboptimal results will be obtained. In order to remedy this and possible inconsistencies in local ties, a post processing correction strategy was proposed by the project to reduce apparent height differences between post processed GPS data and terrestrial measurements such as levelling. These discrepancies occur when unnecessarily tropospheric delays are estimated between co-located stations, or when tropospheric constraints between co-located stations are not taken into account.

The project's strategy was based on the analytical relation between tropospheric delay and the station height of approximately 1:–3 summarised in the Bermuda triangle. A corresponding correction factor  $\delta_U^T$  can be derived either analytically or empirically from the analysis of short baselines (R24) and it is site-dependent (e.g. cut-off, geographic location, satellite visibility) but stays relatively constant over time and for that reason can be calibrated. The correction factor strategy was successfully applied by the project to co-located stations and successfully reduced height discrepancies from the cm-level to some millimetres. This means that all baselines in a regional network can be solved as ionosphere-free solutions with estimated tropospheric delays independently from their baseline length. However, the difference between single-frequency (L1) and dual-frequency, ionosphere-free solutions remains a systematic offset that has not yet been remedied.

### 3.2.3 Influence of the first 50 cm

In GNSS applications with accuracy requirements at the millimetre level, multipath can be denoted as one of the accuracy limiting factors. In particular errors arising from the antenna near-field, which is often approximated by the first 50 cm around the antenna, are critical, as they can change the whole antenna phase characteristics or can lead to long-periodic errors causing a non-zero mean distributed and modelled bias in the estimated parameters (R25).

In order to analyse the influence of antenna near-field effects in the positioning domain, a measurement campaign was performed by the project at the EDM calibration baseline site of the University of Armed Forces in Munich (R26). The GNSS measurements were performed under optimal GNSS conditions, i.e. a nearly multipath-free environment and a nearly free horizon, as all baseline pillars were placed on an earth mound, 3 to 4 metres above the surrounding surface level, and there are no obstacles in the vicinity of the antenna,. Furthermore, reference values for distance and height with superior accuracy were available (R27).

During the measurement campaign seven pillars were equipped with different antenna set-ups, for example spacers with lengths of 20, 40 and 60 cm were used to increase the distance between the top of the pillar and the GNSS antenna. In another antenna set-up, three kinds of geodetic antennas were used (Trimble Zephyr Geodetic, Trimble Zephyr 2 and Leica AT504GG Choke Ring). In order to account for their individual phase centre characteristics, all antennas were calibrated for their phase centre offsets (PCO) and phase centre variations (PCV) in the anechoic chamber of the University of Bonn (as part of Researcher Excellence Grant UBO) (R28). Eight observation sessions of at least 4 hours' duration were performed, leading to an entity of 162 observed baselines.

All baselines were processed using a DD approach and the resulting distance and height components were compared to the reference values of the baseline site. In Figure 14 the differences for the height component are shown.

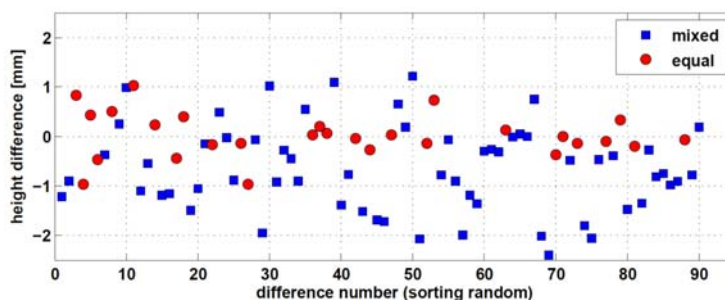


**Figure 14.** Height differences from the reference values (R27) for *equal* and *mixed* antenna-spacer combinations

The blue squares in figure 14 denote differences with mixed antenna-spacer combinations and the red dots denote equal combinations respectively. In Table 1 the mean differences and their standard deviations are displayed for both the distance and height component. The analysis of the project’s results reveals that no influence of a specific spacer type could be detected. However, it was noted that in case of completely identical antenna set-ups (case equal) at both pillars a higher accuracy level could be reached than using different antenna set-ups (case mixed). Due to the excellent GNSS conditions at the baseline site, the long observation durations and the usage of individually calibrated antennas, the deterioration of the accuracy was ascribed to the different near-field situations in the mixed case and lead to the conclusion that a similar antenna set-up leads to similar near-field effects at both pillars and this enables the minimisation of the effect during the double differencing process in the baseline estimation (R29).

Distance component	mean [mm]	$\sigma$ [mm]
Equal	0.14	0.31
Mixed	-0.21	0.53
Height component	mean [mm]	$\sigma$ [mm]
Equal	0.02	0.46
Mixed	-0.65	0.87

**Table 1.** Mean difference values and standard deviations for *equal* and *mixed* antenna-spacer combinations

### 3.2.4 Obstruction

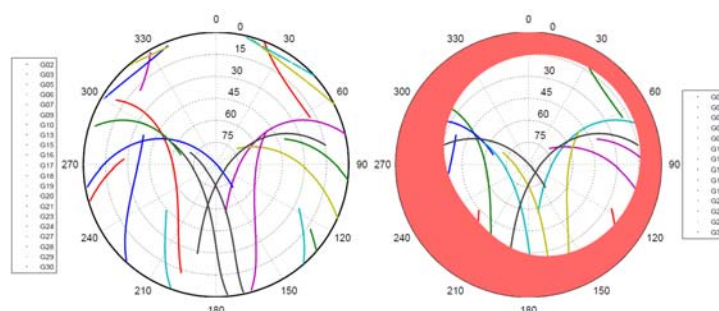


**Figure 15.** Skyplots before (left) and after simulation (right) of scenario *mining*.

Obstacles in the signal path of GNSS satellites lead to a shadowing of the signals which in turn leads to a deterioration of satellite geometry. To analyse the influence of satellite obstructions on the accuracy of GNSS measurements, numerical simulations were performed by the project on GNSS observations that were observed in on otherwise optimum surrounding (R25). In order to gain preferably realistic results, four real expectable shadowing scenarios, i.e. (1) wall, (2) tree, (3) canyon and (4) mining, were defined and simulated. All four scenarios were characterised by boundary values for azimuth and elevation. In the simulation step of the analysis, azimuths and elevations of all visible satellites were determined during a single point positioning. Afterwards the satellites passing the shadowed areas were excluded from the GNSS observation files. In

Figure 15 skyplots of the original observations (left) and after the simulation of scenario *mining* (right) are shown for one observation session. The red area on the right hand side of Figure 15 denotes the shadowed area. After the simulation the baseline estimation was carried out using a standard DD approach and the results, separated in distance and height, were compared to nominal values which had superior accuracy (R26). In Table 2 the mean values and standard deviation of the differences are shown for all scenarios. For comparison purposes the values for the original non-shadowed case are shown as scenario *Ref*. In addition the respective mean Dilution of Precision (DOP) values are listed as a standard measure for the quality of the satellite geometry.

Scenario	Distance component [mm]		Height component [mm]		Mean DOP values		
	x	$\sigma$	h	$\sigma$	P	H	V
Ref	0.14	0.31	0.02	0.46	1.3	0.8	1.0
Wall	0.23	0.41	0.09	0.46	2.1	1.4	1.6
Tree	0.07	.038	0.07	0.46	1.5	1.0	1.1
Mining	0.15	0.38	0.32	0.87	3.4	1.6	3.0
Canyon	0.21	0.40	0.13	0.60	4.2	2.2	3.5

**Table 2.** Mean values and standard deviations of height and distance component and mean DOP values for obstruction scenarios.

The comparison to the non-shadowed case reveals that the accuracy of both the distance and height component are unaffected by the simulated obstructions. Only the precision of the scenarios mining and canyon decreased slightly and the same holds true for the quality of the satellite geometry. In the case of shortened observation durations down to 1 hour and in case of very high DOP values of 7 or higher, the accuracies stay at the same high level below 1 mm. Therefore, it cannot be presumed that the deteriorated satellite geometry is compensated by longer observation durations.

During the simulation of the shadowing scenarios only the satellite geometry was altered, while the quality of the GNSS observations was not manipulated. Due to the optimum GNSS conditions during the data collection, the quality was very high and the observations were not subject to systematic errors, such as multipath or diffraction. However, in reality scenarios such as this would not be the case, since obstructions usually are accompanied by these systematic effects. Therefore it can be hypothesised that far-field multipath effects and signal distortions are more critical than poor satellite geometry and that an approximation of the position accuracy by simply multiplying the measurement accuracy and the respective PDOP value is not sufficient. This statement contradicts common knowledge on obstructions and therefore further work is required before it can be proven (R29).

### 3.2.5 Optimum processing strategy for field measurements

The project also investigated the processing of short baselines using different setups in order to find the metrologically optimum processing strategy for short baselines (< 200 m). The GNSS (here GPS data) processing was carried out using the Bernese GNSS Software version 5.2 and DD solutions of 24 hour sessions were processed with varying carrier frequency, ionosphere and troposphere models and the antenna calibrations. The GPS distances were compared to the traceable reference distances measured using EDM.

The initial processing setup was based on L1 carrier frequency, ten degree cut-off angle and five second sampling interval. The final satellite orbit products provided by the IGS were used and the ambiguities were fixed using the SIGMA algorithm. The two troposphere models were tested with and without tropospheric gradients and the ionosphere effects were tested using either CODE's global ionosphere model or without the use of any model. The test procedure consisted of processing at least three daily solutions using L1 and L3 together with three different antenna calibrations (two individual calibrations and type calibration).

Based on test processing the following strategy was identified by the project as metrologically optimum for baselines shorter than 200 m; L1 double difference observables should be processed using individually calibrated antennas and standard atmospheric models. Ionosphere modelling is not recommended for the

distances shorter than 200 m, and tropospheric gradients describing the local variability of the wet component of the troposphere do not have a realistic meaning on short distances.

These results showed that one millimetre accuracy for baseline length is achievable from 24 hour data using the proposed optimum processing strategy. Half millimetre level changes in distance may occur depending on observation conditions and the antennas in use, but more data is needed to separate the signals from circumstances and antenna calibrations. An accuracy of one to two millimetres can also be achieved with shorter sessions in good conditions. Adding data by using both L1 and L2 frequencies and increasing the data interval to one second may improve the accuracy, but a systematic improvement was not found in such tests.

### 3.2.6 Conclusions

GNSS-based distance metrology is used ubiquitously. While its flexibility is an advantage of this technology, it suffers from uncertainty influences such as signal delays due to the signal traversing the troposphere and ionosphere, and satellite obstruction or signal distortions such as multiple reflections due to the vicinity of the receiver antenna. These influences are impossible to control and difficult to quantify. Therefore, to derive recommendations for optimum measurement strategies and for a sound measurement uncertainty assessment, individual uncertainty contributions were studied and isolated (as far as possible).

Fibre optics were used to synchronise the receiver clocks of two GNSS receivers and this 'common clock' approach eliminated the need to determine the clock as a free parameter. Thus, an unperturbed access to other parameters should have been theoretically possible but, in practice, the receiver electronics were very sensitive to the local environment and this could not be eliminated. Nevertheless, the project successfully demonstrated that the fibre optic approach enabled high resolution height measurements which is important for the monitoring of critical buildings such as bridges.

In addition to this, the optimum processing strategy for the linked parameters height, receiver clock and tropospheric delay was investigated using the standard GNSS analysis approach. With this, a correction strategy was successfully applied to co-located GNSS stations reducing height discrepancies from the centimeter-level to the millimeter-level.

The importance of symmetry in the measurement set up was underlined through outdoor studies on the effect of mounting GNSS antennas on geodetic pillars and studies of typical obstruction scenarios. In the case of symmetrical set ups (same antenna types and mounting, in a similar environment), absolute and standard deviations below 0.5 mm could be achieved, even with additional obstructions. These unexpected results indicate that satellite obstruction itself does not substantially affect measurement uncertainty.

Finally, the project investigated a practical approach for the assessment of uncertainties in GNSS-based distance metrology. The results showed that deviations from reference coordinates taking into account the uncertainty of these reference coordinates and the observed standard deviation were a good indication of the achievable measurement uncertainty for specific configurations and measurement times.

In conclusion, although, a general method for millimetre uncertainties in GNSS could not be produced, the project improved the quantification of relevant uncertainty contributions, and suggested improvements for reducing measurement uncertainties in GNSS-based distance metrology.

### 3.3 Femtosecond laser-based long distance metrology

The spectrum of a femtosecond laser consists of thousands of optical frequencies (wavelengths). The frequency difference between these frequencies is equal to the repetition rate of the pulsed laser, which is about 100-1000 MHz, depending on the particular laser. By phase-locking the repetition rate to a time standard, the whole ‘comb’ of frequencies can be stabilised, typically with a relative uncertainty of  $10^{-11}$  in 1 s averaging time. As a consequence, the distance between the emitted pulses is also stabilised at this level, providing a direct link to the SI definition of the metre.

Prior to this project, measurement concepts that exploited the unique spectral properties of frequency combs, were merely demonstrated on lab table dimensions. Therefore, given the potential of frequency combs, this project pursued objective 3:

*“New concepts for the application of femtosecond laser-based many-wavelength interferometry to long-distance metrology with a targeted relative measurement uncertainty significantly better than  $4 \times 10^{-7}$  under controlled environments.”*

Two different fundamental measurement approaches to access the phase information of multiple modes were pursued, as well as a spectroscopic approach for the compensation of the refractive index. Substantial effort was also given to the development of various approaches for repetition rate multiplication (equivalent to comb mode filtering) as a prerequisite for the realisation of the two fundamental measurement approaches.

#### 3.3.1 Approaches to mode filtering

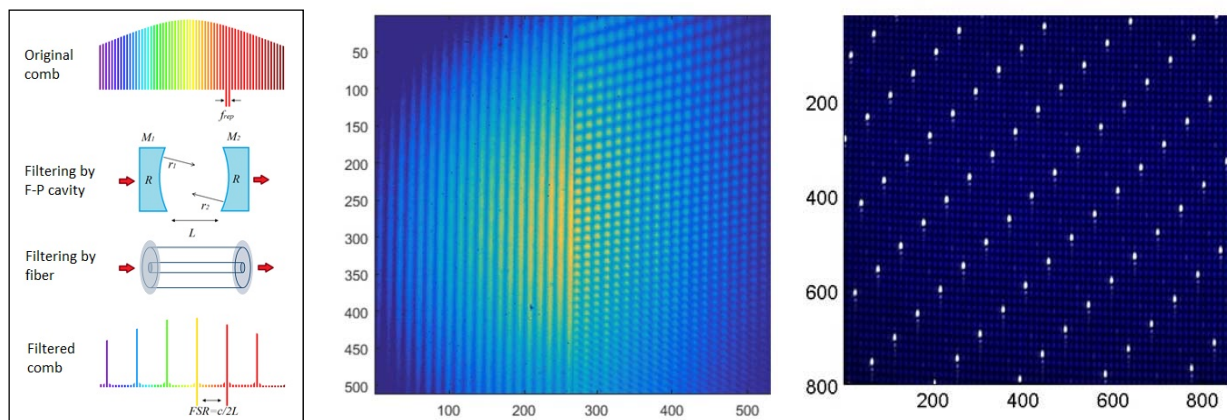


**Figure 16.** Left: schematic of the unfiltered comb spectrum, the two approaches of comb mode filtering, and filtered comb spectrum. Middle: measured spectrum of TU Delft frequency comb by VIPA spectrometer, left side – original 250 MHz spaced modes, unresolvable by spectrometer are shown as continuous lines, right side – spectrum filtered by fiber showing 1 GHz spaced individual comb modes as dots. Right: spectrum of VSL frequency comb measured by VIPA spectrometer, blue dots represents original 1 GHz spaced comb modes, white dots represents modes selected by Fabry-Perot cavity with spacing 41 GHz.

Frequency comb mode filtering is important when the resolution of a spectrometer used for distance measurement is not high enough to resolve individual comb modes. In this project, comb mode spacing of seed frequency combs were realised by optical resonators which were used to filter out any unwanted comb modes.

The first approach (R30) using free space optics, was designed and developed at VSL, and based on two dielectric mirrors with low dispersion ( $GDD < 20 \text{ fs}^2$ ) and high reflectivity  $R = 99.0 \%$ . The mirrors had a diameter  $d = 12.7 \text{ mm}$  and a radius of curvature of  $r = 50 \text{ mm}$  and formed a Fabry-Perot cavity with adjustable length/mode spacing. One of the mirrors was equipped with a piezoelectric ceramic transformer (PZT) adjuster for stabilisation of the cavity length to the chosen frequency comb mode spacing by a dither locking technique. Both mirrors together with other optical components such as mode-matching lenses, beam-splitters and fiber couplers were mounted on a transportable breadboard and an example of the achieved mode filtering is given in figure 16.

The second approach, was designed and developed at ISI (as part of a Researcher Mobility Grant), and based on a filter cavity which consisted of a single optical fibre with deposited reflection layers on both fibre ends. The chosen fibre was characterised by a low chromatic dispersion around 1550 nm wavelength and 40 nm thick silver reflection layers. The fibre was mounted in a cage holding system which consisted of a cage with two fibre connectors mounted on transportable breadboard. The length of tested fibre was 10.24 cm, which corresponds to a mode spacing of 1 GHz, given the refractive index of the fibre core of approximately 1.5. The length can be slightly modulated and stabilised to a frequency comb by a PZT adjuster attached to one of the fibre connectors.

### 3.3.2 Homodyne many-wavelength interferometry over macroscopic distances

In a first approach to exploit the spectral properties of frequency combs for absolute distance interferometry, the project analysed the comb spectrum using a high potential spectrometer, based on a combination of an etalon and a grating (R31). The resolution of the spectrometer was high enough that individual comb modes of a spacing of 1 GHz could be spectrally resolved, as shown in Fig. 17 where each dot represents a (different) optical frequency.

A Michelson interferometer was used (as per conventional interferometry), but the comb light was sent into the interferometer and instead of a conventional detector a high resolution spectrometer was used, and from this, the interference of the wavelengths could be observed from the camera (see Figure 17) and the distance retrieved from the interference pattern in a two-step process. In the first step the distance is derived from the phase change as a function of wavelength (spectral interferometry), using the very accurate frequency scale as defined by the repetition frequency. In the second step the knowledge of each wavelength (about 9000 in this case) was used in addition, potentially leading to further reductions of the measurement uncertainty.

To investigate the accuracy of the method, the project compared the comb based scheme with conventional interferometry. An agreement within 0.5  $\mu\text{m}$  for distances up to 50 m ( $10^{-8}$ ) could be demonstrated (R32), which is better than the targeted uncertainty of better than  $4 \times 10^{-7}$  under controlled environments (see Figure 17). An important advantage of the comb based technique is that the range of non-ambiguity is of the order of 15 cm, which is huge compared to single wavelength interferometry ( $< 0.5 \mu\text{m}$ ). Therefore, a simple course pre-measurement is sufficient to measure absolute distances with high accuracy.

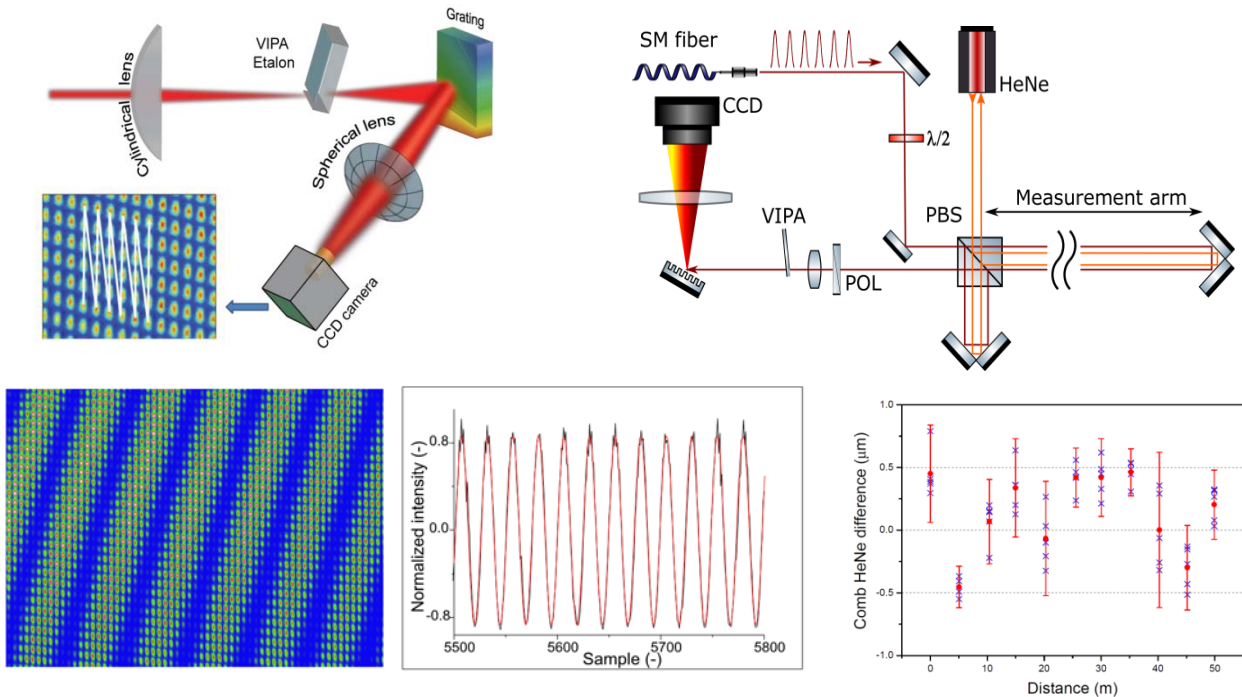


**Figure 17.** TOP. Left: high resolution spectrometer based on a virtually imaged phase array and a grating, resolving individual comb modes as dots on a CCD camera. Right: schematic of the setup for distance measurement. BOTTOM. Left: typical interferometry pattern. Middle: Reconstructed phase change as a function of frequency. Right: distance measurement with comb and HeNe laser compared.

In a second approach, distance measurement with a filtered frequency comb was investigated. Comb filtering can be needed if the wavelengths are too close to be resolved, even with a high resolution spectrometer as described above. Furthermore, if the mode-spacing is increased to values of approximately 50 GHz, even a simple array spectrometer may be sufficient for distance measurement. VSL and ISI (as part of a Researcher Mobility Grant) investigated this latter case and demonstrated agreement within  $10^{-8}$  with a HeNe laser for distances up to 50 m, using a filtered comb with a 56 GHz repetition rate.

The measurement range of this method was only fundamentally limited by the comb linewidth, essentially permitting distance measurements up to thousands of kilometres, which may lead to applications in e.g. inter-satellite distance determination. However with the rapid development of smaller and cheaper frequency comb lasers, it is anticipated that the measurement methods can be implemented in a wide range of distance measurement systems in the near future.

### 3.3.3 Heterodyne frequency-comb based interferometry

Another concept for a multi-wavelength interferometer based on heterodyne phase detection of individual comb lines was inspired by the MSTAR demodulation method “Modulation Sideband Technology for Absolute Ranging” by Lay *et al.* (R33). In the MSTAR demodulation method two frequency combs of different repetition rates are generated as modulation sidebands by phase modulating a single narrow-linewidth, frequency stabilised laser. The combs are then used as local oscillator and signal beams requiring a coherent offset frequency lock between them. The interferometer is realised by splitting the signal comb to serve both the measurement and reference arms of the interferometer. The measurement and reference beams are mixed with the local oscillator frequency comb, in order to gain the distance related phase information. The generated interference signals are then sampled and processed to determine the unknown absolute distance. As both combs consist of many, well defined wavelengths or frequency comb modes, respectively, parallel phase detection is possible without the need for high-speed photodetectors and processing electronics. With the extracted phase information at many frequency comb modes, a wide chain of synthetic wavelengths can be realised leading to a large dynamic range for absolute distance measurement.

While the larger synthetic wavelengths were used to unwrap the phase information of shorter synthetic wavelengths, the final measurement uncertainty was determined by the shortest synthetic wavelength only. The former stems from adjacent comb modes, whereas the latter originates from the comb modes at the far ends of the spectrum. Therefore, a broad bandwidth providing a large amount of comb modes is the most favourable. In this case i.e. a broad bandwidth several synthetic wavelengths of the same order are generated in parallel, such that the phase measurement results can be understood as multiple individual measurements of the same distance and therefore this enables averaging and the reduction of the measurement uncertainty even further.

In a proof-of-principle experiment cavity-enhanced electro-optic frequency comb generators (CEFCGs) were used to refine the MSTAR approach of (R33) and extend the comb bandwidth to 300 GHz consisting of 21 modes. In this experimental setup the sidebands were generated by an electro-optic generator placed within an optical cavity leading to higher-order comb modes due to multiple passes through the modulator. Through the seeding of two such CEFCGs with a single external-cavity diode laser, two coherent combs with repetition rates around 9.2 GHz differing by 5 kHz could be realised. This source was then used to develop a parallel phase detection of multiple comb modes in order to combine a macroscopic range of non-ambiguity with interferometric resolution. The principle for this heterodyne detection scheme and multi-channel digital lock-in phase detection was described in detail in Yang *et al.* (R34). With this approach a relative measurement uncertainty of  $5.3 \times 10^{-7}$  at a measurement distance of 20 m could be demonstrated using 15 comb modes and 7 synthetic wavelengths of the 8<sup>th</sup> order for averaging under laboratory conditions. However, it should be noted that the synthetic wavelengths used for averaging need to be carefully considered to avoid mutual cancellation due to redundant phase information. This preliminary (proof-of-principle experiment) study showed a highly promising uncertainty scaling of the overall measurement result with an affordable optical source, but the small bandwidth of the electro-optic comb pair limited the final measurement uncertainty to the micrometre level.

Femtosecond lasers have already been deployed as optical sources in so-called dual-comb interferometry and feature a significantly larger spectral bandwidth in the order of several THz with thousands of stable and well-defined modes (R35)-(R37). However, two commercial broad band frequency combs are highly cost-intensive and typically only have small repetition rates or a too narrow mode spacing, for such an application. To overcome these issues a tuneable dual-comb-generator based on a coupled pair of Fabry-Perot filtering cavities was developed by the project (R38). Seeded by a single commercially available fibre-based optical

frequency comb with a stabilised carrier envelope offset frequency, two coherent combs of different mode spacing in the GHz band were generated and subsequently used as a local oscillator and signal beam for heterodyne interferometry. This repetition rate multiplication was achieved by selectively filtering out certain comb modes of the seeded laser with a Fabry-Perot resonator whose free spectral range matched a multiple integer of the laser's repetition rate. The minimal repetition rate difference of the filtering cavity doublet was then determined by the initial repetition rate of the seed laser source, and the offset frequency lock between the two combs induced by different frequency shifts from separate acousto-optic modulators. The realisation of this dual comb generator required the development by the project of a sophisticated stabilisation scheme of two cavities, depending on the desired absolute repetition rate, the repetition rate differences and the absolute wavelength of the frequency combs. Although cavity mode filtering lead to a large power loss, which had to be compensated for by optical amplification, down-converted beat note signals between individual comb modes was still detected, the prerequisite for the heterodyne multi-wavelength scheme achieved. Phase-detection, however, could not be achieved in the lifetime of the project, however further by the involved partner is on-going.

### 3.3.4 Comb-based spectroscopic refractivity compensation

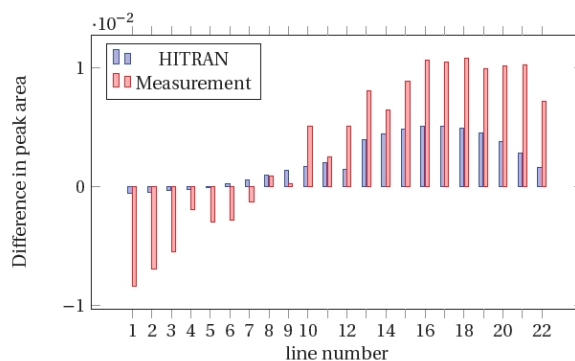


**Figure 18:** The difference in peak height for HITRAN data and measurement when changing the temperature from 24.6°C to 29.6°C.

Temperature changes in a gas lead to a change of refractive index, as can be seen from Edlén's equation, as well as to a change of absorption, as shown in figure 18. When determining the temperature of a gas using absorption measurements, it is possible to determine the refractive index and the project tried to explore the spectroscopic measurement of the temperature using a frequency comb as source (capable of probing multiple absorption lines simultaneously in principle), i.e. intrinsic refractivity compensation combined with the interferometric distance measurement approaches described above.

For assessing the potential of the method, several measurement schemes were investigated. In one such set up for measuring the temperature of CO<sub>2</sub> in a gas cell was developed in a laboratory setting (figure 19) and measurements were taken at two different temperatures. A reference image was taken with an evacuated and a vacuum filled cavity and the spectrum was then normalised, i.e. divided by the baseline value, in order to achieve a transmission of 1 outside of the absorption lines. Several methods were used to determine whether it was possible to retrieve temperature information and the most consistent method was found to be multi peak Lorentzian fitting which showed that the measurement data and the HITRAN reference follow the same trend. Another set up was developed to measure CO<sub>2</sub> absorption in ambient air for determination of temperature. This was done to simulate the effect of outdoor measurement campaigns and the experimental setup was implemented in the basement of the Technical University of Delft (as part of Researcher Excellence Grant TU Delft) and had a length of 640 m. Due to water vapor (H<sub>2</sub>O) having overlapping absorption lines with a broad range of CO<sub>2</sub> absorption lines in the laser bandwidth, a comparatively weak CO<sub>2</sub> line had to be selected, and vibrational stability and turbulence in the optical path length were not sufficiently low to derive meaningful results. Thus the technique appears to be promising but further optimisation of the set up, measurement protocol and analysis techniques are needed.

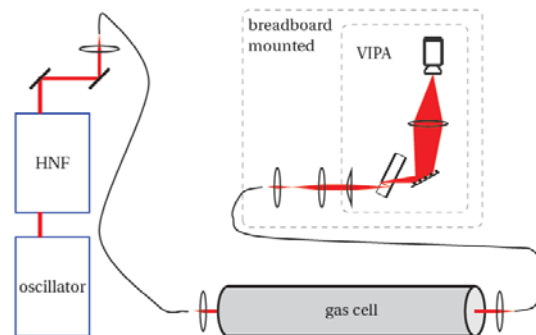


**Figure 19:** The highly nonlinear fiber (HNF) broadens the spectrum to wavelength regions that are not covered by the laser oscillator. The fibers serve as apertures and simplify guidance of the beam between laser output, gas cell and spectrometer. The spectrometer is mounted on an aluminum breadboard.

### 3.3.5 Conclusions

Since their invention in the last decade, optical frequency fibre combs have been advocated as ideal sources for high accuracy length measurements. They provide multiple laser modes with frequencies that can be directly locked to reference clocks in the radio frequency regime, and thus directly to the SI definition of the metre. However, prior to this project, commercially available fibre combs were characterised by low repetition frequencies which complicated their use for length metrology applications. Therefore, the project studied several approaches to address this, such as mode filtering by air-spaced or fibre based Fabry-Perot cavities. From the results a design for a novel broad band dual-comb generator was produced which can be used as a potential source for length metrology applications, as well as being applied to spectroscopic applications.

Heterodyne multi-wavelength interferometry as a fast detection technology was also investigated by the project. It was successfully used to demonstrate a relative measurement uncertainty of  $5.3 \times 10^{-7}$  (0.53 mm) for a measurement distance of 20 m, for cavity-enhanced electro-optic frequency combs.

In conclusion, in terms of length measurement, spectral interferometry proved to be the most successful method with deviations from a counting interferometer below  $1 \mu\text{m}$  up to 50 m, corresponding to a relative measurement uncertainty of  $2 \times 10^{-8}$ . This is the first time that spectral interferometry has been successfully applied over such distances.

### 3.4 Immediate contributions to surveying practice

Surveying is an engineering discipline performed every day across Europe. The central objective of this project was to foster the traceability chain in surveying in order to provide metrological tools for this discipline and to address requirements for accuracy. For the project to generate substantial impact in the field, however, it was necessary to reach out to the many professional surveyors in this field. This motivated objective 4 of the project:

*“To develop solutions to improve state-of-the-art surveying practice, ranging from field-capable optical standards with relative uncertainties of  $10^{-7}$  for long-distance baseline calibrations, over refined guidelines for the calibration of both EDM and GNSS-based distance meters, up to an extensive inter-comparison of major primary geodetic baselines in Europe.”*

#### 3.4.1 Field inter-comparison of instruments and baselines

The optical standards developed in the project were verified under field conditions. This was performed using three of the most stable and best characterised baselines in Europe. In Table 3 the available data sets are summarised from the various field measurement campaigns. All raw data contained the distances and the atmospheric conditions: temperature, air pressure and relative humidity.

The raw data sets were jointly analysed. To do this, each instrument was firstly, separately adjusted to detect blunders and to control the priori stochastic model. This was followed by a joint adjustment with all instruments with scale and additive parameters, to check the additional parameters and to determine relative weights of instruments. Finally, an adjustment was performed based on all instruments introducing significant scale unknowns to determine final coordinates of the pillars and from this step a final set of coordinates was derived. Thus, for each reference baseline i.e. PTB, Nummela, and Munich a set of final coordinates was determined, which consisted of pillar coordinates. The corresponding standard deviations of these values was in the range of 0.1 mm or even better and demonstrated the high quality of the achieved results. The joint analysis of the data sets also linked the scales of the three baselines and established a core of SI traceable and internationally validated reference baselines in Europe.

A more detailed analysis of the instruments and experimental devices on the PTB baseline indicated that there may be a remaining scale difference between the Mekometer ME5000 and the other instruments. Additionally, for the new laser distance systems i.e. the Telediode and TeleYAG systems (see sections 3.1.1 and 3.1.2) the internal standard deviation was expected to be in the range of 0.1 mm, but this was unable to be proven by the observation data sets, mainly due to existing atmospheric influences.

**Table 3.** Baseline data sets and instrument accuracy

Instrument\Baseline	PTB	Munich	Nummela
Kern ME 5000	July 2014	October 2014	October 2015
Leica $\mu$ -Base	July 2014		
TeleYAG	November 2015	July 2015	September 2015
TeleDiode	June 2015		April 2016

#### 3.4.2 Data digging at the PTB 600 m baseline

Based on experience, surveyors have developed “good practice rules” to be adhered to when the highest accuracies are targeted. “The good geodetic hour” before dawn is often recommended for this purpose, or at least a measurement with a high cloud coverage. Monitoring the environmental conditions simultaneously at the start and target point of the measurement is also considered as favourable. However, a measurable parameter for the quality of the measurement conditions or at least a distinction of observations under more or less favourable environmental conditions was missing prior to the start of this project.

The dense sensor network at the PTB 600 m baseline has been running continuously since its installation in 2011, and has collected a huge set of environmental observation data which is spatially resolved and can be attributed to various times-of-day. This dataset could be complemented by additional meteorological data from a station of the German weather service DWD located in the vicinity of the baseline. Therefore this huge data set was systematically reviewed for correlations and systematics by the project. Temperature, proved to be an

unsuitable parameter for the quality of the weather conditions, whilst solar irradiance showed a strong correlation with the homogeneity of the observed environmental conditions. The results of this study supported and helped to refine “common knowledge” in surveying as well as the development of good practice guides (see section 3.4.5).

### 3.4.3 EDM calibration on baselines

Due to current regulations surveyors and survey authorities are obliged to calibrate their distance measuring equipment (EDM) to determine the calibration parameters: a scale factor and an additional constant. For this reason a measurement campaign is usually carried out on a reference baseline. Therefore, the project compiled recommendations for high level calibrations EDMs on baselines based on the experience gathered and analysis tools developed during the various high accuracy measurement campaigns during the project (see section 3.4.1), the analysis of the large environmental dataset available at the PTB 600 m baseline (see section 3.4.2). The resulting good practice guide can be downloaded from the project website and recommendations were based on:

- The reference baseline consists of pillars in a straight line whose coordinates should be known traceable to the SI definition of the metre with a sound measurement uncertainty assessment according to the GUM. The pillars dispose of a high precision centring system and the measured distance depends on the atmospheric conditions along the signal path, for example a difference of 1 °C in temperature causes a difference of 1 mm in a 1 km distance; therefore a dense sensor field to record the atmospheric conditions is desirable.
- To determine the calibration parameters the measured distance can be compared with the distances calculated from the pillar coordinates. The advantage of this approach is that the uncertainties of the pillar coordinates and the centring system can be ignored. In a model, realised in newly developed software by the Technical University of Braunschweig in a researcher excellence grant, the coordinates are not fixed, but the accuracy of the pillars is taken into account and a least square adjustment of the pillar coordinates and the instrument parameters can be determined. Using these instrument parameters future measurements can then be corrected. The newly developed software supports different input formats of distance measurements and an automatic detection of outliers can be implemented.
- To achieve optimal results, the measurements must be carried out very carefully. The tribrachs have to be levelled and the difference between the instrument and prism heights has to be measured and should not exceed 15 mm. The clock of the instrument also has to be carefully controlled, as well as the atmospheric conditions. The temperature, the air pressure and the relative humidity must be measured during the measurement campaign, as a minimum at the station and prism position. Further to this, the configuration of the atmospheric parameters in the instrument must be controlled and adopted to the current weather conditions or set to the reference atmospheric condition of the instrument; (in this case the reduction of the distances is carried out in the software).

### 3.4.4 The revolver test field concept for antenna parameter verification

The reference point of GNSS positioning and distances is the GNSS antenna reference point (ARP), which is located usually on the bottom of the antenna. Existing calibration tables contain corrections for the phase observations which relate the phase centre to the ARP. However, the phase centre of the GNSS antenna, cannot be solely determined from the antenna design to the sub millimetre level. Instead its position depends on signal reception direction and the local surroundings, and can alter over time. For this reason, GNSS antennas for high accuracy applications need to be calibrated by sophisticated automated methods in order to determine the phase centre offset and the phase centre variation as a function of the direction of the incoming signal. For the surveyor, it is important to verify the validity of these calibrations on site under actual ‘field’ measurement conditions and surroundings. Therefore, the project developed the “revolver test” which uses antenna swapping and rotating in order to verify the calibration tables of antennas.

As part of the “revolver test” verification, the residual offsets of the antennas are determined after application of the calibration values. The group of antennas which will later be used together in the field is then tested at the same time in order to get the relative residual offsets between the antennas. The residual offsets should be zero if the calibration tables are valid, thus there should not be any antenna related biases in the coordinate

results of the sessions. The significance of estimated residual offsets were tested with the null hypothesis “no (i.e. zero) residual offsets” and a decision on the validation of the calibration table made.

The principle of determining the residual offsets is to circulate antennas in pillars, as between sessions the only change should be the location of individual antennas or the orientation of an antenna. Thus receivers, centring devices and cables should be the same in every session at each pillar. The environmental changes should be insignificant and atmospheric changes between sessions should be predominantly eliminated in double differences in data processing. In the revolver test field which was realised at the geodetic fundamental station of Metsähovi the height differences of the pillars were small and distances between the pillars were short, 2-5 m, Finland. Figure 20 shows the six session observation plan for three antennas and three pillars. Full 24 hour sessions are preferable and the test sites and pillars should be stable with guaranteed visibility to the satellites.

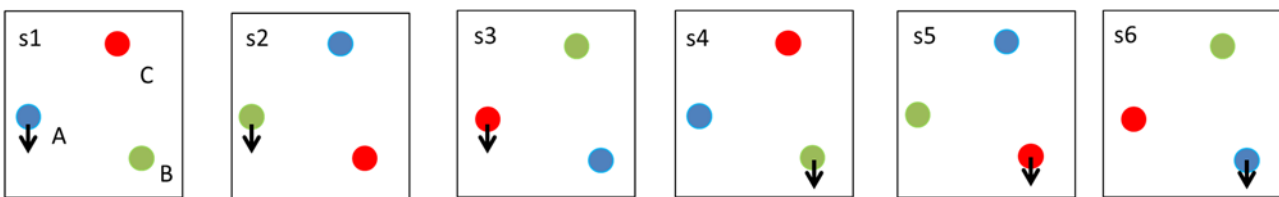


**Figure 20.** Principle of set up with three antennas (blue, green and red) and three pillars (A, B, C). The arrow shows the pillars at which the antenna is oriented to the South instead of the usual North orientation.

Using the “revolver test” each session is processed separately for all frequencies using reliable GNSS software without estimating site specific troposphere parameters. The preferable elevation cut off angle in processing is 15 degrees and the free network solutions of sessions with their covariance matrices are combined in residual offset estimation. In the combination model the unknown parameters are site coordinates ( $X_i$  and  $X_j$ ) and antenna specific parameters, i.e. residual offsets ( $O_p$  and  $O_q$ ) of the antenna. Estimated residual offsets explain the differences between session solutions due to the antenna and the functional relationship between the observations  $\Delta X_{ij}$  and unknown parameters is

$$X_j - X_i + R_{j_s} O_p - R_{i_s} O_q = \Delta X_{ij}.$$

$R_{j_s}$  and  $R_{i_s}$  are the rotations around the vertical. This is a matrix representation for a single vector. If the number of vectors in session is number of pillars minus one then the number of equation in residual offset estimation is

$$n_{equations} = n_{sessions} \cdot 3 \cdot (n_{pillars} - 1)$$

The revolver test design, procedure and analysis was realised at the geodetic fundamental station of Metsähovi, Finland where several GNSS antennas were used for high accuracy monitoring. Simulations and test measurement performed at Metsähovi showed that depending on the number of antennas, pillars and sessions, residual offsets could be resolved at the sub-millimetre level.

### 3.4.5 Good practice guides for high accuracy GNSS-based distance measurements

The project experimentally investigated various influences on the measurement uncertainty of GNSS-based distance measurements and conclusions on good practice in terms of suitable preparatory measures for the hardware, as well as for suitable mounting and experiment design were drawn in addition to strategies for tropospheric corrections in non-trivial cases or for a feasible, and metrologically sound estimates of the measurement uncertainty. These conclusions are relevant for high accuracy GNSS-based distance measurement and therefore to make these results accessible to surveyors in the field, a good practice guide was compiled on high accuracy GNSS-based distance measurements, which is available for download from the project’s website (R39).

### 3.4.6 Conclusions

One of the major outcomes of the project was the linking of three European primary geodetic baselines in Finland and Germany via an extensive field study using different transfer standards such as the TeleYAG and TeleDiode systems developed in objective 1, as well as commercial state-of-the-art devices. Following their comparison, these primary geodetic baselines can now provide European surveyors with SI traceable calibration of their devices with low uncertainty.

The project also developed the sophisticated “Revolver” field test for the validity of GNSS antenna calibration parameters. This test is based on measurement campaigns with multiple antennas. By suitable antenna swapping and rotating, and using high-level analysis, the test procedure is sensitive to 0.1 mm level for the absolute residual offsets of each antenna for the North and East component and relative residual offsets for the ‘Up’ component. Therefore, a verified tool to test GNSS equipment in the field with reduced instrumentation is now available for European surveyors.

Finally, two good practice guides were produced by the project with the aim of reducing uncertainty contributions in GNSS-based distance metrology and in electronic distance meters baseline calibrations. These good practice guides are available for end-users on the project’s website <http://www.emrp-surveying.eu/emrp/2984.html>.

In conclusion, the project was able to improve the metrological core of European surveying and to provide measurement and verification strategies for daily work in surveying. These combined outputs contribute to improving the state of the art of surveying practice.

### 3.5 Local tie metrology at geodetic fundamental stations

Surveyors, geodesists, and also earth scientists describe and compare their measurements often in a common local or global frame of reference like the ITRF. Reference frames play thus an important role for the SI traceability of these observations. Origin and scale of these systems are determined by a common analysis of various space geodetic observations like GNSS (predominantly GPS), VLBI, Satellite Laser Ranging (SLR), Laser Lunar Ranging (LLR), and Doppler Orbitography and Radiopositioning Integrated by Satellites (DORIS). However, a critical step is the transformation of individual observations at co-location sites, so-called geodetic fundamental stations, into a joint coordinate system. The vectors connecting the reference points of the various instruments are called “local tie vectors” and are of utmost importance for this step. They are determined by surveying methods at these geodetic fundamental stations and their uncertainty is a prime candidate for explaining discrepancies between different space geodetic methods reported in previous ITRF combinations. The project therefore pursued objective 5

*“To investigate different approaches to real-time monitoring of local ties at geodetic fundamental stations, both experimentally and theoretically. Thus, fundamental metrology for the Global Geodetic Observing System (GGOS) will be developed with an overall target to reduce the uncertainty of reference frames to 0.1 mm.”*

#### 3.5.1 Uncertainty assessment of local tie networks

A GUM conformal assessment of the measurement uncertainty is the prerequisite for sound discussion of potentials and limitations of state-of-the-art measurement technologies and potential improvements. However, due to the complexity of the measurement, a stringent GUM conformal uncertainty assessment had not been conducted prior to this project. In two pilot studies (R40) and (R41), the determination of the “GPS local tie” at Metsähovi was investigated by this project using four methods: two theoretical methods: (1) the variance propagation in least squares adjustment and the (2) Monte Carlo Method (MCM) and two empirical (3) time series of the repeated local tie measurements and (4) the comparison of GPS local tie and the terrestrial local tie. The investigated monitoring network consisted of the IGS GPS point and the trajectory points of the GPS antennas on the edge of the VLBI antenna main reflector. The measurand was the vector between the GPS antenna reference point of the IGS GPS antenna and the VLBI telescope reference point. Input values were the coordinates of the trajectory points and the telescope position angles.

In the variance propagation method in least squares estimation the inverse of the normal equation included the variances of the reference point coordinates as a function of the geometry of the trajectory points and the covariance matrix of the trajectory point coordinates and the VLBI antenna position angles. In the MCM method, the distribution of uncertainties of the input values which are measurands of the kinematic post processing of the GPS observations were assessed first, before the influence of the GPS processing on these quantities was estimated. Sets of trajectory coordinates could then be simulated and the resulting distribution of reference point coordinates derived. The variances of local tie vector components calculated from repeated local ties finally gave the empirical assessment of the overall uncertainty. For comparison, the time series of reference point observations (figure 21) or the difference of the reference point coordinates achieved by two different measurement techniques could in principle serve as an indicator of the achievable measurement uncertainty of the local tie vector.

Semi-major axes of the error ellipsoid of the reference point coordinates from least squares adjustment from MCM and from the time series (25 sessions) were 0.44 mm, 0.97 mm and 1.71 mm respectively. The distances between the terrestrial determination and GPS determinations of the VLBI telescope reference point in the dedicated campaigns during the project were 3 mm and 2 mm and a magnitude of 1 to 2 mm for the achievable measurement uncertainty of local tie measurements was determined.

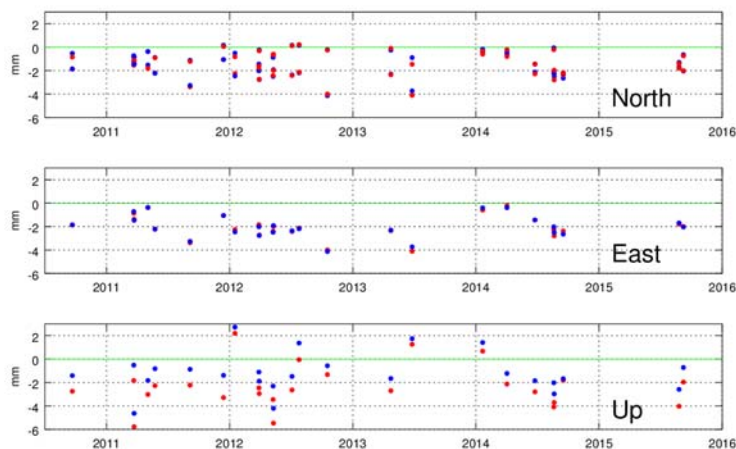


**Figure 21.** Scattering of the GPS local tie vector components in time series. The raw data set was analysed using two different phase centre calibration sets for GPS antennas.

### 3.5.2 Local-tie adapted 3D metrology

VLBI or SLR antennas are macroscopic systems of extensions of metres up to tens of metres. Since they have to aim at and track radiation sources and reflectors they can be dynamically oriented. But due to different gravitational loads for different device orientations, and to environmental effects like thermal expansion, the location of the reference point and thus, the magnitude of the local tie vector changes constantly. Several approaches were explored by the project in order to improve the monitoring of the location of the reference point.

In the first approach, a GNSS based monitoring system was established at the geodetic fundamental stations in Metsähovi, Finland and in Onsala, Sweden. The measurement method was based on two GNSS antennas attached permanently on the edge of the VLBI dish. The GNSS antenna points rotate around the elevation axis which rotates around the azimuth axis. The reference point is the projection of the elevation axis in the azimuth axis. Axes are not perpendicular and they do not intersect. The reference point coordinates are estimated after the kinematic post processing of the GNSS observations. The point cloud of antenna points with telescope position angles were observations in reference point estimation and GNSS antennas should be individually calibrated and precise orbits of the satellites should be used in processing.

One problem of this GNSS-based measurement approach turned out to be a significant loss of data due to multipath effects and blockage of the visibility by the radio telescope antenna, as well as ambiguous resolution in the post processing of data. However the advantages of this approach are that it can generate an almost continuous dataset and can be performed fully automated, while not interfering with the normal use of the radio telescope. Furthermore, unlike with optical methods, a local area network is not necessary and the local tie is determined directly in the ITRF without the need of a Helmert transformation.

As part of an alternative approach, robotic total stations were mounted on surveying pillars to monitor the position of the geodetic reference points of the Metsähovi and Onsala VLBI telescopes in topocentric reference frames. The system was controlled by the specialised HEIMDALL software package (R42) and the newly thus installed HEIMDALL system is now capable of operating several robotic total stations in concert with geodetic VLBI telescopes to the extent that full automation is within reach. The highest grade total stations were used and the system performance was found to be limited by the geometry of the setup, i.e. not the instrument specifications. Although automatic when in operation, the deployment of the HEIMDALL systems were quite labour intensive due to hardware restrictions and required some further development to become an integral part of the Space Geodetic Observing system. These boundaries are primarily due to the number of available robotic total stations at each site, but in the longer term the capability to incorporate the robotic stations with the computers running the telescope schedule files need to also be taken into account. Nevertheless, the HEIMDALL system has proven capable of determining the geodetic reference point in the topocentric frame with sufficient precision for foreseeable geodetic needs and the project has shown that the limiting case for accuracy is the orientation with respect to the global frame.

Other approaches of the project included mounting a high-grade terrestrial laser scanner in the quadropod of the Onsala 20 m telescope in order to quantify the elevation dependent deformation of the telescope's reflector. In the Onsala case, the reflector deformation implicated a rather large systematic impact on the observations and indicate that the influence of deformation related systematic errors of VLBI observations are larger than previously anticipated. It is also possible that the current understanding of contributing error sources need to be modified, although to what extent this is a single station effect or a general behaviour is not yet known and will require further investigation.

### 3.5.3 GNSS-VLBI baseline measurement

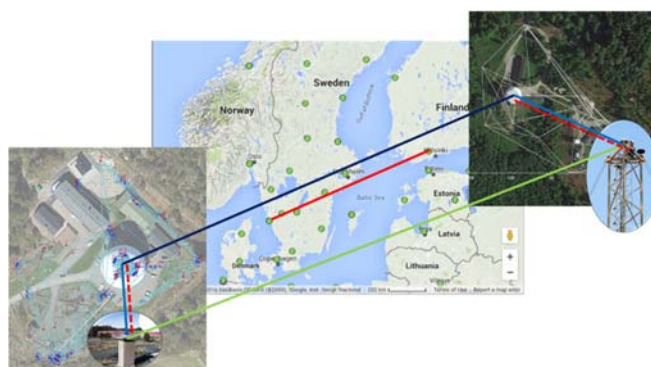


**Figure 22.** Sketch of the IGS – IVS baseline comparison set up. The baselines between the geodetic fundamental stations of Metsähovi, Finland, and Onsala, Sweden, were determined both by VLBI (dark blue) and GNSS (green) observations. They are compared using the local tie vectors derived either by GNSS observations (red dashes) or terrestrial observations (light blue).

The economic effort and human expertise for the installation of a 3D capable real-time local tie monitoring system is substantial. Thus to justify such an installation proof of the benefit is necessary. Therefore the project undertook a baseline verification experiment between the two geodetic fundamental stations of Metsähovi and Onsala was performed in order to compare the GNSS-based to the HEIMDALL derived local tie vector.

The baseline experiment between the Metsähovi and Onsala sites consisted at each end of one IGS station, one International VLBI Service for Geodesy and Surveying (IVS) station, one terrestrial tie monitoring system and one telescope-mounted GNSS tie consisting of two antennas. The electromagnetic environment of the telescope put constraints on the signal propagation to the telescope-mounted GNSS antennas and ordinary processing schemes were not feasible. Therefore two different GNSS processing schemes were developed, and compared with the terrestrial ties in order to evaluate which more appropriately representing the telescope reference movements. The GNSS antennas were permanently installed on the telescopes, whereas only Metsähovi has purchased a terrestrial total station for permanent use.

In August 2015, a joint VLBI and GNSS observation campaign was performed by the project with the goal to compare IGS and IVS baselines using differently generated local tie vectors (figure 22). The availability of the VLBI data was initially delayed due to limitations of the correlator, which is the central facility that processes the extremely faint signals of the observations. All data is now available, and the data analysis has commenced, however, due to the fact that the new generation geodetic VLBI telescopes are currently being installed at Onsala, the data analysis was delayed. The data set is particularly pertinent to the Metsähovi and Onsala stations that are situated in a postglacial isostatic adjustment region where ground movements are slow but predictable. Therefore the analysis is part of a longer term commitment at both sites, and the processing and evaluation will continue beyond the end of this project.

### 3.5.4 Conclusions and outlook

Local tie vectors connect the reference points of different space-earth measurement observing systems. Their monitoring networks are highly complex, but are crucial for the generation of a global reference system which forms the basis for GPS-based navigation or global observations of climate-induced changes, for example. This project theoretically investigated existing networks and derived complex models for uncertainty

propagation. Different approaches were used to estimate the overall achievable measurement uncertainty of contemporary local tie vector monitoring in the order of 1 – 2 mm. The project also installed GNSS-based and terrestrial real-time 3D observation systems at the geodetic fundamental stations of Onsala, Sweden and Metsähovi, Finland. The observation systems are capable of monitoring reference points during system operation in real-time. They can therefore directly measure unexpected position changes induced, for example, by temperature expansion. This is expected to reduce the uncertainty of local tie vectors, in the longer term and provides a promising 'new' approach.

In conclusion, the project established analysis tools to assess the measurement uncertainty of local tie measurements. This is necessary to make quantifiable advances in the measurement technology. The 3D observation systems installed in the project will be studied in the community in the next few years. The goal of 0.1 mm, as inspired by geodetic roadmap papers needs further work and will require a much larger effort from the surveying community in forthcoming years.

### 3.6 Summary of major research results and project outputs

The project covered a vast field of technologies and methods and has improved long-distance metrology with:

- The project's TeleYAG system has demonstrated its capability as novel primary standard for the calibration of geodetic baselines with relative uncertainties at the  $10^{-7}$  level, based on intrinsic refractivity compensation. PTB is working towards implementing this as a high level calibration service in the near future.
- The project's TeleDiode system has demonstrated very low standard deviations in outdoor use and is well advanced in terms of transportability, stability and user-friendliness. CNAM is currently discussing the commercialisation of the system and thus, a reliable, high-accuracy transfer standard might be available in the nearer future to the surveying community.
- Spectroscopic thermometry as alternative technology to intrinsic dispersive refractivity compensation was successfully demonstrated by the project for the first time under outdoor conditions over a significant distance of several hundreds of metres.
- The optical distance measurement methods developed by the project were shown to approach the accuracy limit determined by turbulence. Methods were successfully developed to study turbulence and its impact and from this applicable rules of thumbs were derived.
- In a unique effort, the manifold uncertainty influences on sub-millimetre accuracy GNSS-based distance metrology have been studied by the project and from this best practice recommendations for high accuracy measurements were deduced and published.
- Although common-clock GNSS turned out to induce more problems than originally anticipated, its value for kinematic applications was demonstrated by the project.
- The treatment of tropospheric influences when dealing with GNSS networks of mixed, i.e. shorter and longer distances was shown to be vital for real-life applications in surveying.
- Study of the influence of the first 50 cm of the antenna surrounding and the influence of obstruction showed the importance of symmetric set ups in GNSS based distance metrology. Results indicated that, in contrast to current knowledge in the field, satellite obstruction only has a minor impact on measurement uncertainty compared with the multipath associated with the obstructing features.
- The revolver test developed in the project can be used as tool for end users to verify the calibration status of their GNSS antennas.
- In the field of femtosecond laser-based distance metrology, the project explored several strategies and dispersive interferometry using spectrally resolved comb mode lines achieved the best results, even up to 50 m. This technology has clear potential for future application in length metrology although for long distance metrology in uncontrolled environments, a number of issues like beam stabilisation still need to be overcome.
- Fundamental work for the establishment of real-time monitoring of local ties was performed by the project and the refurbishment of the Finnish geodetic fundamental station at Metsähovi was used to establish a real time monitoring network. A joint VLBI and GNSS campaign between the Finnish and the Swedish geodetic fundamental stations was successfully performed.
- The project team has successfully disseminated its results to the surveying community with two workshops and the 3rd Joint International Symposium on Deformation Monitoring (JISDM) 2016, Vienna, jointly organised by the International Federation of Surveyors (FIG) and the international association of geodesy (IAG) hosted two dedicated sessions for the presentation of the project's results
- Finally, the DVW, the association of professional surveyors in Germany, has declared its interest in publishing the project's GNSS and EDM guidelines in their pre-standard series.

#### 4 Actual and potential impact

Traceability of long distance measurements in surveying remains a highly challenging field. This project developed scientific and technological solutions for high-accuracy long distance metrology. Lower uncertainty levels were successfully met by the project, including reducing the measurement uncertainty of optical distance measurements in air well below 1 mm over a distance of 1 km. Many of these outputs are already available to end users to improve traceability in surveying, geodesy and earth sciences.

##### Dissemination of results

The project has had 35 publications accepted and/or published so far, predominantly in high impact journals such as Scientific Reports, Optics Letters, Journal of Applied Geodesy, Review of Scientific Instruments or Measurement Science and Technology. The international length metrology community was addressed by contributions to the specialised MacroScale conference 2014, in Vienna, Austria, and the 17<sup>th</sup> International Congress of Metrology 2015 in Paris, France, and the time and frequency community by contributions to the Precise Time and Time Interval Meeting (PTTI) 2016 in Monterey, USA, and the 5<sup>th</sup> International Colloquium – Scientific and Fundamental Aspects of the Galileo Programme 2015, Braunschweig, for example. The results were also presented to and discussed by leading international length metrologists at open EMRP/EMPIR workshops organised by EURAMET Technical Committee Length (TC-L) at Braunschweig and Delft in 2013 and 2016, respectively.

Furthermore, as a special forum to continue the discussion and to draw conclusions on the future of this vital field, project participants have initiated a dedicated five-day workshop in 2017 on “Trends and developments in Laser Based Distance Metrology”. This event is funded by the Lorentz center in Leyden, Netherlands and will bring the leading experts from all over the world together.

Aside from fundamental science, special emphasis was put on the establishment of strong links to the large stakeholder community during the project. In particular, a stakeholder advisory board with representatives from surveying, device manufacturers, space geodesy and high energy physics regularly monitored the project and provided feedback.

Wider communication with the surveying community was also achieved by presentations at stakeholder conferences, e.g. at the International Association of Geodesy Scientific Assembly 2013 in Potsdam, Germany, the International Earth Rotation and Reference Systems Service (IERS) Workshop on Local Surveys and Co-locations 2013, in Paris, or the IUGG General Assembly 2015 in Prague, Czech Republic. Furthermore, the project was invited to present its work on local tie metrology at the International Very Long Baseline Interferometry (VLBI) Service 2016 General Meeting in South Africa. Moreover, the project coordinator was invited to present the outcomes of the project to the association of professional surveyors in Germany, the “Deutscher Verein für Vermessungswesen (DVW)” in June, 2016, in Hanover, at the 153. DVW seminar on “Quality Assurance of Geodetic Measurement and Evaluation Methods”. It should be noted that the latter event shows that the research performed indeed reached out to actual challenges in professional surveying.

In addition to this, the project presented itself and its progress concisely at two dedicated occasions to the stakeholder community. The project organised the “1st Workshop on Metrology for Long Distance Surveying” on November 21, 2014 at project partner IPQ, in Portugal. 25 presentations were given by the consortium and external researchers to an audience of more than 50 external experts and end-users from all over the world.

As a final event, the 3rd Joint International Symposium on Deformation Monitoring (JISDM) 2016, Vienna, jointly organised by the International Federation of Surveyors (FIG) and the international association of geodesy (IAG) hosted two dedicated sessions for the presentation of the project’s results. Thus, the project’s results were presented to a large audience of approximately 150 international monitoring experts and the corresponding proceedings are available at

[https://www.fig.net/resources/proceedings/2016/2016\\_03\\_JISDM\\_programme.asp](https://www.fig.net/resources/proceedings/2016/2016_03_JISDM_programme.asp)

The project’s publications as well as many presentations are available for end-users on the project website [www.emrp-surveying.eu](http://www.emrp-surveying.eu)

##### Standardisation

One of the most effective ways to achieve the overall goal of the Surveying project, a substantial improvement of traceability in long-distance metrology in surveying and geodesy, is the implementation of project results in novel standards and good practice guides in the field. Two Good Practice Guides (objective 4) were published by the project:

1. Good practice guide for the calibration of EDMs on baselines
2. Good practice guide for the calibration of GNSS-based distance meters under different conditions

They can be freely downloaded from the project webpage under <http://www.ptb.de/emrp/2984.html>.

The consortium discussed its outcomes with a number of major standardisation bodies in surveying, including the ISO/TC 172/SC6 "Optics and photonics - geodetic and surveying instruments" and DIN NA 005-03-04 AA "Geodätische Instrumente und Geräte (SpA zu ISO/TC 172/SC6)" (the German standardisation mirror committee to ISO/TC 172/SC6). In particular, the project's GNSS work (objective 2) was presented to both committees. One outcome of this was that a new DIN working group was formed for the development of a GNSS-oriented standard, in which the project coordinator participated. The project's sophisticated "Revolver" field test (objective 4) is also being discussed with the DIN working group as a candidate for an advanced procedure for future standardised enhanced field tests of geodetic GNSS antennas. A proposal for an approximate GUM conformal treatment of the measurement uncertainty derived from the work objective 2 is also being considered for this standard.

Moreover, the association of professional surveyors in Germany, the DVW, has declared an interest in the project's good practice guides on GNSS-based distance metrology and EDM baseline calibrations (objective 4). Currently the guides are being reviewed and editorial changes are being performed. The final versions may be published in the DVW's pre-standard series "DVW Merkblätter". These pre-standards have a substantial impact on the surveying community and are intended as a fast communicator of research results into daily practice in the field. They are often also the basis for future revisions of existing standards and novel standards on ISO level.

Further to this, the project developed close collaborations with standardisation bodies in geodesy, in particular in the field of local tie metrology. A member of the consortium was even elected head of the International Earth Rotation and Reference Systems Service (IERS) Working Group on Site Survey and Co-location. Conclusions from the project's local tie studies (objective 5) were fed into the development of a best practice guide for core sites (geodetic fundamental stations) in the Global Geodetic Observing System [http://cddis.gsfc.nasa.gov/docs/2015/SiteRecDoc\\_Rev2\\_D3.4.pdf](http://cddis.gsfc.nasa.gov/docs/2015/SiteRecDoc_Rev2_D3.4.pdf). Thus the project's results will, in the future, contribute to future realisations of the ITRF. This will also improve the quality of the European Terrestrial Reference System 1989 ETRS89 and as a consequence, the traceability of any measurement performed within this reference frame e.g. in earth sciences like climatology.

Finally, the project also supported and initiated standardisation efforts in the metrology community. Based on conclusions derived by work on objective 2, project members contributed to a draft documentary standard by a the GNSS working group of the Consultative Committee for Time and Frequency (CCTF) at the Comité international des poids et mesures (CIPM). Moreover, in its 2016 meeting, EURAMET TC-L encouraged the project team to revise its good practice guide on EDM calibration (objective 4) formally so that it can be considered as a novel EURAMET Calibration Guide

#### Early impact on traceability in surveying and geodesy

Project outcomes are being taken up by several organisations:

- Discussions are underway with a French SME about the commercialisation of the one wavelength TeleDiode system (from objective 1) for high-end long distance measurements.
- The use of optical cavities combined with mode-locked femtosecond lasers (objective 3) for the length characterisation of piezoelectric actuators is being discussed with the Czech company MESING who specialise in the design and manufacture of length measuring devices for the engineering industry.
- A specialised software tool developed in the project for the analysis of the data from the comparison of the three European primary geodetic baselines (objective 4) will be made available to the surveying community.
- PTB will use the data from the comparison from objective 4, to establish a Calibration and Measurement Capability (CMC) service for the long-distance calibration of EDMs.
- CNAM will make the TeleDiode prototype (from objective 1) available to the French national geodesy and cartography institute IGN for use in a practical survey in order to demonstrate the TeleDiode prototype's accuracy and productivity. Joint studies between CNAM and IGN are currently on-going.

- CNAM has developed an all-fibred EDM with surprisingly high performance at low cost. This is expected to be available within the next year.
- The 3D real time local tie monitoring system (from objective 5) will be permanently installed and used at the geodetic fundamental stations of Onsala, Sweden, and Metsähovi, Finland. It will contribute to the International Terrestrial Reference Frame (ITRF), a set of coordinates located on the Earth's surface.
- At Metsähovi, the project's sophisticated "Revolver" test field (objective 4) was integrated into the local tie network and is now routinely used there to check antennae deployed for local tie monitoring of the ITRF.

### *Potential future impact*

The project's outcomes will help surveyors and researchers in geosciences face the challenge of measuring distances over several hundred metres up to kilometres with lower uncertainties. The potential fields of application are landslide monitoring, the monitoring of critical sites like future carbon dioxide or nuclear waste repositories, and for ensuring the accurate positioning of agricultural machinery such as combine harvesters and thus helping to control European agricultural subsidies.

The results of the GNSS studies have triggered further studies at PTB regarding the optimum set up of the GNSS system for time transfer. These studies may lead to a refurbishment and optimisation of this important installation in the future.

PTB intends to improve transportability of TeleYAG technology further to offer calibration service of primary baselines for legal metrology purposes in legal metrology.

Scientific conclusions on local tie metrology will influence local tie monitoring at geodetic fundamental stations of the GGOS in future.

## 5 Website address and contact details

A public website for the project is available at: <http://www.emrp-surveying.eu>

The contact person for the project is Florian Pollinger, PTB, [florian.pollinger@ptb.de](mailto:florian.pollinger@ptb.de)

## 6 List of publications

- [1]. Appleby G, Behrend, Bergstrand S, Donovan H, Emerson C, Esper J, Hase H, Long J, Ma C, McCormick D, Noll C, Pavlis E, Ferrage P, Pearlman M, Saunier J, Stowers D, Wetzel S, GGOS Requirements for Core Sites, CDDIS: NASA's Archive of Space Geodesy Data (2015)

[http://cddis.gsfc.nasa.gov/docs/2015/SiteRecDoc\\_Rev2\\_D3.4.pdf](http://cddis.gsfc.nasa.gov/docs/2015/SiteRecDoc_Rev2_D3.4.pdf)

- [2]. Bergstrand S, Collilieux X, Dawson J, Haas R, Long J, Pavlis EC, Sauniér J, Schmid R, Nothnagel A, Resolution on the nomenclature of space geodetic reference points and local tie measurements, Proceedings of the Symposium on Reference Frames for Applications in Geosciences (REFAG2014), International Association of Geodesy Symposia, ISBN 978-3-319-45628-7

<https://www.iers.org/IERS/EN/Organization/WorkingGroups/SiteSurvey/documents.html>

- [3]. Bosnjakovic A, Pollinger F, Meiners-Hagen K, Improving the traceability chain in geodetic length measurements by the new robust interferometer TeleYAG, Journal of Trends in the Development of Machinery and Associated Technology: 19, 117-120 (2015)

[http://www.tmt.unze.ba/zbornik/TMT2015Journal/030\\_Journal\\_TMT\\_2015.pdf](http://www.tmt.unze.ba/zbornik/TMT2015Journal/030_Journal_TMT_2015.pdf)

- [4]. Droste S, Grebing C, Leute J, Raupach SMF, Matveev A, Hänsch TW, Bauch A, Holzwarth R and Grosche G, Characterization of a 450-km Baseline GPS Carrier-Phase Link using an Optical Fiber Link, New J. Phys. 17 083044 (2015)

<http://dx.doi.org/10.1088/1367-2630/17/8/083044>

- [5]. Guillory J, Garcia-Marquez J, Alexandre C, Truong D and Wallerand JP, Characterization and reduction of the amplitude-to-phase conversion effects in telemetry, Meas. Sci. Technol. 26 (8), 084006 (2015)  
<http://dx.doi.org/10.1088/0957-0233/26/8/084006>
- [6]. Guillory J, Smid R, Garcia Marquez J, Truong D, Alexandre C, Wallerand J P, High resolution kilometric range optical telemetry in air by Radio Frequency phase measurement, Rev. Sci. Instr. 87, 075105 (2016)  
<http://dx.doi.org/10.1063/1.4954180>
- [7]. Guillory J, Wallerand J P, Truong D, Smid R, Alexandre C, Towards kilometric-range Distance measurements with air refractive index compensation, Proceedings of the 3rd Joint International Symposium on Deformation Monitoring, (JISDM), Vienna, (March 30 - April 1, 2016) (2016)  
[http://www.fig.net/resources/proceedings/2016/2016\\_03\\_jisdms\\_pdf/nonreviewed/JISDM\\_2016\\_submission\\_27.pdf](http://www.fig.net/resources/proceedings/2016/2016_03_jisdms_pdf/nonreviewed/JISDM_2016_submission_27.pdf)
- [8]. Haensel A, van den Berg S, Urbach P, Bhattacharya N, Beam Path Temperature Determination for Long Distance Measurements, Proceedings of the 3rd Joint International Symposium on Deformation Monitoring (JISDM), Vienna, (March 30 - April 1, 2016) (2016)  
[http://www.fig.net/resources/proceedings/2016/2016\\_03\\_jisdms\\_pdf/nonreviewed/JISDM\\_2016\\_submission\\_38.pdf](http://www.fig.net/resources/proceedings/2016/2016_03_jisdms_pdf/nonreviewed/JISDM_2016_submission_38.pdf)
- [9]. Heunecke O, Die neue Neubiberger Pfeilerstrecke, zfV 140 (6), 357-364 (2015)  
<http://dx.doi.org/10.12902/zfv-0086-2015>
- [10]. Jokela J, Kallio U, Koivula H, Poutanen M, NLS's Contribution in the JRP SIB60 "Metrology for Long Distance Surveying," Proceedings of the 3rd Joint International Symposium on Deformation Monitoring (JISDM), Vienna, (March 30 - April 1, 2016) (2016)  
[http://www.fig.net/resources/proceedings/2016/2016\\_03\\_jisdms\\_pdf/nonreviewed/JISDM\\_2016\\_submission\\_43.pdf](http://www.fig.net/resources/proceedings/2016/2016_03_jisdms_pdf/nonreviewed/JISDM_2016_submission_43.pdf)
- [11]. Krawinkel T, Lindenthal N, and Schön S, Scheinbare Koordinatenänderungen von GPS-Referenzstationen: Einfluss von Auswertestrategien und Antennenwechseln, zfV 139, 252-263 (2014)  
<http://dx.doi.org/10.12902/zfv-0027-2014>
- [12]. Lesundak A, Smid R, Voigt D, Cizek M, van den Berg SA, Cip O, Proc. SPIE 9450, Photonics, Devices, and Systems VI, 94501L (6 January 2015) (2015)  
<http://dx.doi.org/10.1117/12.2074415>
- [13]. Leute J, Bauch A, Schön S, Krawinkel T, Common Clock GNSS-baselines at PTB, Proceedings of the 3rd Joint International Symposium on Deformation Monitoring (JISDM), Vienna, (March 30 - April 1, 2016) (2016)  
[http://www.fig.net/resources/proceedings/2016/2016\\_03\\_jisdms\\_pdf/nonreviewed/JISDM\\_2016\\_submission\\_102.pdf](http://www.fig.net/resources/proceedings/2016/2016_03_jisdms_pdf/nonreviewed/JISDM_2016_submission_102.pdf)
- [14]. Meiners-Hagen K, Bosnjakovic A, Koechert P and Pollinger F, Air index compensated interferometer as a prospective novel primary standard for baseline calibrations, Meas. Sci. Technol. 26 (8), 084002 (2015)  
<http://dx.doi.org/10.1088/0957-0233/26/8/084002>
- [15]. Mildner J, Meiners-Hagen K, Pollinger F, Dual-frequency comb generation with differing GHz repetition rates by parallel Fabry-Perot cavity filtering of a single broadband frequency comb source, Meas. Sci. Technol. 27 (7), 074011 (2016)  
<http://dx.doi.org/10.1088/0957-0233/27/7/074011>

- [16]. Niemeier W, Tengen D, Uncertainty assessment in geodetic network adjustment by combining GUM and MC simulations, Journal of Applied Geodesy, awaiting publication.
- [17]. Niemeier W, et al, Good Practice Guide: Guidelines for the calibration of EDMs on baselines (2016)  
[http://www.ptb.de/emrp/fileadmin/documents/surveying/Good\\_practice\\_guide\\_for\\_the\\_calibration\\_of\\_EDMs\\_on\\_baselines\\_public\\_v1\\_01.pdf](http://www.ptb.de/emrp/fileadmin/documents/surveying/Good_practice_guide_for_the_calibration_of_EDMs_on_baselines_public_v1_01.pdf)
- [18]. Pires C, et al, Good Practice Guide: Guidelines for the calibration of GNSS-based distance meters under different conditions (2016)  
[http://www.emrp-surveying.eu/emrp/fileadmin/documents/surveying/Good\\_practice\\_guide\\_for\\_high\\_accuracy\\_GNSS\\_based\\_distance\\_metrology\\_public\\_v1.pdf](http://www.emrp-surveying.eu/emrp/fileadmin/documents/surveying/Good_practice_guide_for_high_accuracy_GNSS_based_distance_metrology_public_v1.pdf)
- [19]. Pollinger F, Kupko V, Neyezhmakov P, Poutanen M, Kallio U, Kuhlmann H, Zucco M, Astrua M, van den Berg S A, Schön S, Niemeier W, Merimaa M, Koivula H, Jokela J, Görres B, Meiners-Hagen K, Bauch A and Saraiva F, Metrology for Long Distance Surveying: A Joint Attempt to Improve Traceability of Long Distance Measurements, in C. Rizos, P. Willis (Eds.), IAG 150 Years, Proc. IAG Scientific Assembly in Potsdam, Germany, 1-6 September, 2013, International Association of Geodesy Symposia 143, Springer (2016)  
[http://dx.doi.org/10.1007/1345\\_2015\\_154](http://dx.doi.org/10.1007/1345_2015_154)
- [20]. Pollinger F et al, JRP SIB60 "Metrology for Long Distance Surveying" - a concise survey on major project results, Proceedings of the 3rd Joint International Symposium on Deformation Monitoring (JISDM), Vienna, (March 30 - April 1, 2016) (2016)  
[http://www.fig.net/resources/proceedings/2016/2016\\_03\\_jisdms\\_pdf/nonreviewed/JISDM\\_2016\\_submission\\_16.pdf](http://www.fig.net/resources/proceedings/2016/2016_03_jisdms_pdf/nonreviewed/JISDM_2016_submission_16.pdf)
- [21]. Pollinger F, Mildner J, Köchert P, Yang R, Bosnjakovic A, Meyer T, Wedde M, Meiners-Hagen K, SI-Traceable High Accuracy EDM based on Multi Wavelength Interferometry, Proceedings of the 3rd Joint International Symposium on Deformation Monitoring (JISDM), Vienna, (March 30 - April 1, 2016) (2016)  
[http://www.fig.net/resources/proceedings/2016/2016\\_03\\_jisdms\\_pdf/nonreviewed/JISDM\\_2016\\_submission\\_15.pdf](http://www.fig.net/resources/proceedings/2016/2016_03_jisdms_pdf/nonreviewed/JISDM_2016_submission_15.pdf)
- [22]. Pravdova L, Lesundak A, Hucl V, Cizek M, Mikel B, Hrabina J, Rerucha R, Cip O, Lazar J, Length characterization of a piezoelectric actuator travel with a mode-locked femtosecond laser, Proc. SPIE 9525, Optical Measurement Systems for Industrial Inspection IX, 95254K (June 22, 2015);  
<http://dx.doi.org/10.1117/12.2190745>
- [23]. Schön S, Pham HK, Kersten T, Leute J, Bauch A, Potential of GPS common clock single-differences for deformation monitoring, Journal of Applied Geodesy (2016)  
<http://dx.doi.org/10.1515/jag-2015-0029>
- [24]. Schön S, Pham H K, and Krawinkel, On removing discrepancies between local ties and GPS-based coordinates, International Association of Geodesy Symposia, Springer (2016)  
[http://dx.doi.org/10.1007/1345\\_2016\\_238](http://dx.doi.org/10.1007/1345_2016_238)
- [25]. Schön S, Pham HK, Kersten T, Leute J, Bauch A, Potential of GPS common clock single-differences for deformation monitoring, Journal of Applied Geodesy (2016)  
<http://dx.doi.org/10.1515/jag-2015-0029>

- [26]. Smid R, Hansel A, Pravdova L, Sobota J, Cip O, Bhattacharya N, Comb mode filtering silver mirror cavity for spectroscopic distance, *Rev. Sci. Instr.* 87, 093107 (2016)  
<http://dx.doi.org/10.1063/1.4962681>
- [27]. Tomberg T, Hieta T, Fordell T, Merimaa M, Spectroscopic Inline Thermometry, Proceedings of the 3rd Joint International Symposium on Deformation Monitoring, (JISDM), Vienna, (March 30 - April 1, 2016) (2016)  
[http://www.fig.net/resources/proceedings/2016/2016\\_03\\_jisdms\\_pdf/nonreviewed/JISDM\\_2016\\_submission\\_69.pdf](http://www.fig.net/resources/proceedings/2016/2016_03_jisdms_pdf/nonreviewed/JISDM_2016_submission_69.pdf)
- [28]. van den Berg SA, van Eldik S, and Bhattacharya N, Mode-resolved frequency comb interferometry for high-accuracy long distance measurement, *Sci. Rep.* 5, 14661 (2015)  
<http://dx.doi.org/10.1038/srep14661>
- [29]. van den Berg S, Voigt D, Lesundak A, van Eldik S, Bhattacharya N, Highly Accurate Distance Measurement with a Frequency Comb Laser, Proceedings of the 3rd Joint International Symposium on Deformation Monitoring (JISDM), Vienna, (March 30 - April 1, 2016) (2016)
- [30]. [http://www.fig.net/resources/proceedings/2016/2016\\_03\\_jisdms\\_pdf/nonreviewed/JISDM\\_2016\\_submission\\_20.pdf](http://www.fig.net/resources/proceedings/2016/2016_03_jisdms_pdf/nonreviewed/JISDM_2016_submission_20.pdf)
- [31]. Voigt D, van den Berg S, Lesundak A, van Eldik S and Bhattacharya N, High accuracy absolute distance measurement with a mode-resolved optical frequency comb, *Proc. SPIE 9899, Optical Sensing and Detection IV*, 989906 (2016)  
<http://dx.doi.org/10.1117/12.22273360>
- [32]. Yang R, Pollinger F, Meiners-Hagen K, Tan J and Bosse H, Heterodyne multi-wavelength absolute interferometry based on a cavity-enhanced electro-optic frequency comb pair, *Opt. Lett.* 39, 5834-5837 (2014)  
<http://dx.doi.org/10.1364/OL.39.005834>
- [33]. Yang R, Pollinger F, Meiners-Hagen K, Krystek M, Tan J and Bosse H, Absolute distance measurement by dual-comb interferometry with multi-channel digital lock-in phase detection, *Meas. Sci. Technol.* 26 (8), 084001 (2015)  
<http://dx.doi.org/10.1088/0957-0233/26/8/084001>
- [34]. Zimmermann F, Eling C, Kuhlmann H, Investigations on the influence of Antenna Near-field Effects and Satellite Obstruction on the Uncertainty of GNSS-based Distance Measurements, *Journal of Applied Geodesy*, 53-60 (2016)  
<http://dx.doi.org/10.1515/jag-2015-0026>
- [35]. Zimmermann F, Eling C, Kuhlmann H, Investigations on the Influence of Antenna Near-field Effects and Satellite Obstruction on the Uncertainty of GNSS-based Distance Measurements, Proceedings of the 3rd Joint International Symposium on Deformation Monitoring (JISDM), Vienna, (March 30 - April 1, 2016) (2016)  
[http://www.fig.net/resources/proceedings/2016/2016\\_03\\_jisdms\\_pdf/reviewed/JISDM\\_2016\\_submission\\_17.pdf](http://www.fig.net/resources/proceedings/2016/2016_03_jisdms_pdf/reviewed/JISDM_2016_submission_17.pdf)
- [36]. Zucco M, Pisani M, Astrua M, Characterization of the effects of the turbulence on the propagation of a laser beam in air, *Proc. CIM 2015, 17th International Congress of Metrology Paris*, (September 21, 2015) (2015)  
<http://dx.doi.org/10.1051/metrology/20150013014>

## 7 References

- (R01) F. K. Brunner, K. Kraus, "Kinematics of a deep-seated landslide derived from photogrammetric, GPS and geophysical data", *Engineering Geology* 88, 149 (2006)
- (R02) D. Sahagian et al., "Earth observation: Serving the needs of an increasingly global society", p. 153-196 152 in „Global Geodetic Observing System Meeting the Requirements of a Global Society on a Changing Planet in 2020“, edited by H. P. Plag and M. Pearlman, Springer, Berlin (2009)
- (R03) J. Jokela, P. Häkli, M. Poutanen, U. Kallio, J. Ahola, "Improving Length and Scale Traceability in Local Geodynamical Measurements". Proceedings of the 2009 IAG Symposium "Geodesy for Planet Earth", Buenos Aires, Argentina, August 31 – September 4, 2009. International Association of Geodesy Symposia, Vol. 136, p. 59–66. ISBN 978-3-642-20337-4. (2012)
- (R04) J.-M. Nocquet, A. Walpersdorf, F. Jouanne, F. Masson, J. Chéry, and P. Vernant, "Slow deformation in the Western Alps from a decade of Continuous GPS measurements", Proc. 3rd Intern. Colloquium - Scientific and Fundamental Aspects of the Galileo Programme, 31 August - 2 September 2011, Copenhagen, Denmark (2011)
- (R05) S. A. Khan, J. Wahr, M. Bevis, T. van Dam, "Greenland GPS Network: A Tool to Study Mass Balance of the Greenland Ice Sheet", Proc. 3rd Intern. Colloquium - Scientific and Fundamental Aspects of the Galileo Programme, 31 August - 2 September 2011, Copenhagen, Denmark (2011)
- (R06) G. A. Milne, J. L. Davis, J. X. Mitrovica, H.-G. Scherneck, J. M. Johansson, M. Vermeer, H. Koivula, "Space-Geodetic Constraints on Glacial Isostatic Adjustment in Fennoscandia", *Science*, 291, 2381-2385 (2001)
- (R07) G. Colosimo, M. Crespi, A. Mazzoni, M. Jones, D. Missiaen, "Determination of the CNGS global geodesy OPERA public note", 132, 1-7 (2011)
- (R08) C. Rizos et al., „Maintaining a modern society“, p. 135-152 in „Global Geodetic Observing System Meeting the Requirements of a Global Society on a Changing Planet in 2020“, edited by H. P. Plag and M. Pearlman, Springer, Berlin (2009)
- (R09) N. K. Pavlis and M. A. Weiss, "The relativistic redshift with  $3 \times 10^{-17}$  uncertainty at NIST", Boulder, Colorado, USA, *Metrologia* 40, 66–73 (2003)
- (R10) E. Peik and A. Bauch, "More Accurate Clocks – What are They Needed for?", Special Issue / PTB-Mitteilungen 119, No. 2, 16-24 (2009)
- (R11) S.A. van den Berg, G.J.P. Kok, S.T. Persijn, M.G. Zeitouny, N. Bhattacharya, "Many-wavelength interferometry with thousands of lasers for absolute distance measurement", *Phys. Rev. Lett.* 108, 183901 (2012)
- (R12) Z. Altamimi, "ITRF and Co-location Sites", Proceedings of the IERS Workshop on site co-location, IERS Technical Note No. 33 (2003)
- (R13) H.-P. Plag and M. Pearlman (eds.), "Global Geodetic Observing System Meeting the Requirements of a Global Society on a Changing Planet in 2020", Springer-Verlag, Berlin (2009)
- (R14) R. Gross, G. Beutler, H.-P. Plag, "Integrated scientific and societal user requirements and functional specifications for the GGOS", p. 209-224 in "Global Geodetic Observing System Meeting the Requirements of a Global Society on a Changing Planet in 2020", edited by H. P. Plag and M. Pearlman, Springer-Verlag, Berlin (2009)
- (R15) K. Meiners-Hagen and A. Abou-Zeid, "Refractive index determination in length measurement by two-colour interferometry", *Meas. Sci. Technol.* 19, 084004 (2008)
- (R16) K. Meiners-Hagen, A. Bosnjakovic, P. Köchert, and F. Pollinger, "Air index compensated interferometer as a prospective novel primary standard for baseline calibrations," *Meas. Sci. Technol.* 26, 084002 (2015).
- (R17) K. Meiners-Hagen, T. Meyer, G. Prellinger, W. Pöschel, D. Dontsov, and F. Pollinger, "Overcoming the refractivity limit in manufacturing environment", *Opt. Express* 24, 24092 (2016).
- (R18) Scripps Institution for Oceanography, "Scripps O2 program," [http:// http://scrippsco2.ucsd.edu/index](http://scrippsco2.ucsd.edu/index).
- (R19) T. Tomberg, T. Hieta, T. Fordell, M. Merimaa, "Spectroscopic Inline Thermometry" in proceedings of the 3rd Joint International Symposium on Deformation Monitoring (JISDM), Vienna (2016)
- (R20) T. Tomberg, T. Fordell, J. Jokela, M. Merimaa, T. Hieta, "Spectroscopic thermometry for long distance surveying", *Appl. Opt.* 56, 239 (2017)
- (R21) J. Leute, A. Bauch, T. Krawinkel, S. Schön, "Common clock GNSS-baselines at PTB", Proc. of JISDM 2016 (2016)
- (R22) R. Santerre and G. Beutler, "A proposed GPS method with multi-antennae and single receiver", *Bulletin Géodésique* 67, 210 (1993)

- (R23) S. Schön, K. Hue Pham, T. Kersten, J. Leute, J., A. Bauch, "Common Clock Single-differences for Deformation Monitoring", *J. Appl. Geodesy* 10, 45 (2016)
- (R24) S. Schön, K. Pham, T. Kersten, "On Removing Discrepancies Between Local Ties and GPS-based Coordinates", *Proc. IUGG Prag*, Springer (2016)
- (R25) F. Dilssner, G. Seeber, G. Wübbena, M. Schmitz, "Impact of Near-Field Effects on the GNSS Position Solution", *Proceedings of the 21st International Technical Meeting of the Satellite Division of the Institute of Navigation (ION GNSS 2008)*, Savannah, Georgia, 612 (2008)
- (R26) H. Heister, "Die neue Kalibrierbasis der UniBW München", *Allgemeine Vermessungsnachrichten (AVN)* 10, 336 (2012)
- (R27) O. Heunecke, "Auswertung des Ringversuchs auf der neuen Kalibrierbasis der UniBW München zur Bestimmung der Sollstrecken", *Allgemeine Vermessungsnachrichten (AVN)* 11-12, 380 (2012).
- (R28) P. Zeimetz, H. Kuhlmann, "On the Accuracy of Absolute GNSS Antenna Calibration and the Conception of a New Anechoic Chamber", *Proceedings of the FIG Working Week 2008*, Stockholm, Sweden (2008)
- (R29) F. Zimmermann, C. Eling, H. Kuhlmann, "Investigations on the influence of antenna near-field effects and satellite obstructions on the uncertainty of GNSS-based distance measurements", *J. Appl. Geodesy* 10, 53 (2016)
- (R30) A. Lešundák, R. Šmíd, D. Voigt, M. Čížek, S. A. van den Berg, O. Číp, "Repetition rate multiplication of a femtosecond frequency comb", *Proc. SPIE 9450*, Photonics, Devices, and Systems VI, 94501L (January 6, 2015) (2015)
- (R31) S. A. van den Berg, G. J. P. Kok, S. T. Persijn, M. G. Zeitouny, N. Bhattacharya, "Many-Wavelength Interferometry with Thousands of Lasers for Absolute Distance Measurement", *Phys. Rev. Lett.* 108, 183901 (2012)
- (R32) S. A. van den Berg, S. van Eldik, N. Bhattacharya, "Mode-resolved frequency comb interferometry for high-accuracy long distance measurement", *Scientific Reports* 5, 14661, (2015)
- (R33) O. P. Lay, S. Dubovitsky, R. D. Peters, J. P. Burger, S.-W. Ahn, W. H. Steier, H. R. Fetterman, Y. Chang, "MSTAR: a submicrometer absolute metrology system", *Opt. Lett.* 28, 890 (2003)
- (R34) R. Yang, F. Pollinger, K. Meiners-Hagen, M. Krystek, J. Tan, H. Bosse, "Absolute distance measurement by dual-comb interferometry with multi-channel digital lock-in phase detection", *Meas. Sci. Technol.* 26, 084001 (2015)
- (R35) I. Coddington, W. C. Swann, L. Nenadovic, N. R. Newbury, "Rapid and precise absolute distance measurements at long range", *Nat. Photon.* 3, 351 (2009)
- (R36) S. Yokoyama, T. Yokoyama, Y. Hagihara, T. Araki, T. Yasui, "A distance meter using a terahertz intermode beat in an optical frequency comb", *Opt. Express* 17, 17324 (2009)
- (R37) J. Lee, S. Han, K. Lee, E. Bae, S. Kim, S. Lee, S.-W. Kim, Y. J. Kim, "Absolute distance measurement by dual-comb interferometry with adjustable synthetic wavelength", *Meas. Sci. Technol.* 24, 045201 (2013)
- (R38) J. Mildner, K. Meiners-Hagen, F. Pollinger, "Dual-frequency comb generation with differing GHz repetition rates by parallel Fabry–Perot cavity filtering of a single broadband frequency comb source", *Meas. Sci. Technol.* 27 (2016) 074011
- (R39) The good practice guides are at <http://www.ptb.de/emrp/2984.html>.
- (R40) U. Kallio, M. Poutanen, J. Kallunki, "Uncertainty of daily based local ties", in preparation
- (R41) W. Niemeier, D. Tengen, *Proc. 3rd Joint Internat. Symp. on Deformation Monitoring (JISDM)*, Vienna, (March 30 - April 1, 2016) (2016)
- (R42) M. Lösler, C. Eschelbach, A. Schenk, and A. Neidhardt, "Permanentüberwachung des 20 m VLBI-Radioteleskops an der Fundamentalstation in Wettzell", *ZfV* 135, 40 (2010)